

**KINETIC MECHANISM OF NUCLEOSIDE HYDROLASE FROM
*ESCHERICHIA. COLI***

by

Lencie Plancher

A Thesis Submitted to the
Faculty of the College of Graduate Studies at
Middle Tennessee State University
in Partial Fulfillment of the Requirement for the Degree
of Master of Science in Chemistry

Middle Tennessee State University
May 2016

Thesis committee:

Dr. Paul C. Kline, Major Professor

Dr. Donald A. Burden

Dr. Mary B. Farone

This thesis is dedicated to the following people:

- My parents, Micheline and Lerome Plancher, who instilled in me the inspiration to set high goals and the confidence to achieve them.
- My siblings, Wadeline, Roselande, and Woodly, who have been my emotional anchors through my entire life.
- My cousin Roseline D., who has been a proud and supportive of my work.

ACKNOWLEDGMENTS

Because it takes a village, I would like to express my immeasurable appreciation and deepest gratitude to everyone who have helped me throughout my graduate studies.

First, I would like to thank God, the Lord almighty for filling me with love, strength and blessing me throughout this journey.

My sincere gratitude to my advisor, Dr. Paul Kline. His door was always open whenever I had questions about my research and writing. His great efforts for explaining things clearly and simply to me. I was blessed to have an advisor who has patience, enthusiasm, and inspiration about the subject.

To my committee members: Dr. Donald Burden and Dr. Mary Farone, thank you for their time and carefully reviewed my chapters. Their insightful comments have helped me a lot. I also want to thank Dr. Dwight Patterson for his kind assistance and giving me his wise advice.

A special thanks goes to the instrument support engineer Jessie Weatherly, who spent time teaching me about mass spectrometry. I also want to thank Brock Arivett for introducing me to the CLC drug discovery workbench software. Their help is much appreciated.

I'm grateful to my friends: Geraldine Prophete, Phillip Pulley, Clifford Williams, and France Makabu for all the emotional support, entertainment, and caring. They helped me get through difficult times.

Thanks to the chemistry department for providing me with all the equipment I needed to complete my project.

Finally, I would like to thank my family for all their love, support, and encouragement. My parents Micheline and Lerome Plancher, my grandmother Lucilia Devariste and my sibling Wadeline, Roselande, and Woody Plancher. They have been my constant source of love, strength, and prayer. Special thanks to my cousine Roseline, she has been a great supporter. I love her dearly and thank her for all the advices and words of encouragement.

ABSTRACT

Nucleoside hydrolases are key enzymes that catalyze the hydrolysis of the N-glycosidic bond in nucleosides to allow recycling of the purines and pyrimidines.¹ Inosine-Uridine Nucleoside Hydrolase (IU-NH) of *Crithidia fasciculata* has previously been studied and considered as a potential target for drug design. Although various nucleoside hydrolases have been extensively characterized many aspects of the ribonucleoside hydrolase C (RihC), are unclear. In this study, wild type and mutants of RihC from *E.coli* have been expressed, purified, and analyzed. Gel electrophoresis confirmed the purity and the existence of the proteins as tetramers. The calculated molecular weight based on the amino acid sequence is 32.57 kDa while SDS-PAGE indicated a molecular weight of 33 kDa. Analyzed proteins showed significant activity with the substrate inosine. Turnover number and specific activity were consistent with each other. A 3D structure of RihC from *E.coli* bound with substrate inosine was developed using CLC Drug Discovery workbench software. Interactions between the substrate and residues involved in the active site of the enzyme were identified. A comparison between the known structure of IU-NH from *C. fasciculata* and the modeled RihC from *E.coli* with inosine bound in the active sites was carried out with regard to the interactions between the substrate and the residues in the active site.

TABLE OF CONTENTS

	PAGE
LIST OF TABLES.....	vii
LIST OF FIGURES.....	viii
CHAPTER	
I. INTRODUCTION.....	1
1. Purines and Pyrimidines.....	5
2. Nucleoside Hydrolases.....	5
3. Nucleoside Hydrolases from <i>Escherichia Coli</i>	6
4. Structures Representative of Different Parasitic Groups of Nucleoside Hydrolase.....	7
5. Enzymes.....	13
6. Enzymes Kinetic and Mechanism.....	13
7. Research Goal.....	16
II. MATERIALS AND METHODS.....	17
1. Materials and Reagents.....	17
2. Growth of Recombinant <i>E.coli</i> Cells.....	17
3. Purification of Enzyme.....	18
4. Reducing Sugar Assay.....	18
5. Protein Concentrations.....	19
6. Determination of Enzyme Purity by SDS-PAGE Electrophoresis.....	20
7. HPLC Analysis of Enzyme Activity.....	21
8. Kinetic Activity.....	22

9. Structure Refinement.....	22
III. RESULTS AND DISCUSSIONS.....	25
IV. CONCLUSION.....	48
REFERENCES.....	50

LIST OF TABLES

TABLES	PAGE
1. Typical activity data of wild type.....	31
2. Amino acid changes and their role in rihC.....	33
3. Specific activities of mutants with inosine as substrate used in this study.....	34
4. Kinetic parameters for wild type, and mutants D15, F164, L241, and H233 with inosine.....	34

LIST OF FIGURES

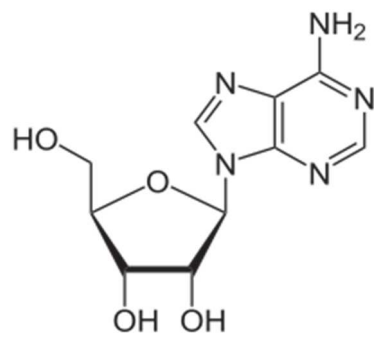
FIGURE	PAGE
1. Structure of nucleosides and nucleotides.....	2
2. The common purine and pyrimidine nucleosides.....	3
3. Structures of <i>syn</i> and <i>anti</i> purine nucleoside conformations.....	4
4. Hydrolysis of adenosine to adenine and ribose.....	7
5. Distinct quaternary structures, tertiary structures, and topologies of <i>Crithidia fasciculata</i> IU--NH (a, c, e) and <i>Trypanosoma vivax</i> IAG-NH (b, d, f).....	10
6. Comparison of the active sites of IU-NH (a, c) in complex with pAPIR and IAG-NH (b, d) in complex with inosine	11
7. Amino acid sequence alignment for 8 selected putative NH proteins.....	12
8. The enzyme- substrate complex (ES).....	13
9. Michealis-Menten equation.....	14
10. Michaelis-Menten kinetic.....	15
11. Standard curve for reducing sugar assay.....	19
12. Standard calibration curve of protein absorbance 595nm.....	20
13. SDS-PAGE standard curve for Precision Plus Protein unstained.....	21
14. Two dimensional structure of inosine.....	24
15. ClustalW comparison of <i>Crithidia fasciculata</i> and <i>E. coli</i> nucleoside hydrolases.....	26
16. Mutant 233 elution profile after passage through a Ni agarose column.....	27
17. Coomassie blue staining of purified wild type and mutants of rihC from <i>E.coli</i>	28

18. Coomassie blue staining of purified mutant 15.....	29
19. Typical protein HPLC chromatogram of wild type enzyme.....	30
20. Typical activity profile of wild type enzyme as a function of reaction time.....	31
21. Kinetic analysis of inosine nucleoside hydrolase (rihC) of Mutant L241.....	35
22. Kinetic analysis of inosine nucleoside hydrolase (rihC) of Mutant H233.....	36
23. Kinetic analysis of inosine nucleoside hydrolase (rihC) of Mutant F164.....	37
24. Kinetic analysis of inosine nucleoside hydrolase (rihC) of Mutant D15.....	38
25. Sequence alignment comparison of IU-NH from <i>Crithidia fasciculata</i> and RihC of <i>E.coli</i>	40
26. Tetramer structure of <i>E.coli</i> RihC.....	42
27. 3D Structure of RihC of <i>E.coli</i> monomer bound to inosine.....	43
28. 3D Structure of RihC from <i>E.coli</i>	44
29. Crystal structure of IU-NH of <i>Crithidia fasciculata</i> bound with substrate inosine.....	45
30. Molecular surface of RihC of <i>E.coli</i>	46
31. Molecular surface of IU-NH of <i>C. fasciculata</i>	47

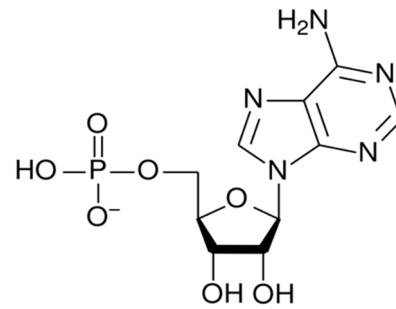
CHAPTER I

INTRODUCTION

Cell growth depends on the contribution by both purine and pyrimidine nucleosides and nucleotides. In all organisms, nucleic acids are the molecules containing the genetic information necessary to sustain life. There are two types of nucleic acids, deoxyribonucleic acid (DNA) and ribonucleic acid (RNA). They are linear polymers composed of nucleotides linked by phosphodiester bonds. RNA directs the synthesis of proteins, while DNA stores the information for protein synthesis². Nucleotides are the building blocks of DNA and RNA consisting of a nitrogenous base (purine or pyrimidine), a sugar (ribose or deoxyribose), and a phosphate group (Figure 1). Nucleosides are formed from a nitrogen base linked by a glycosidic bond to C1' of a sugar (Figure 1). Nitrogenous bases are named by changing the ending of the nitrogen base to *osine* for purines and *idine* for pyrimidines. The most common nitrogen-containing bases in DNA and RNA are cytosine, guanine, adenine, thymine and uracil. (Figure 2). The bases rotate around the glycosidic linkage to a preferred conformation (Figure 3). These preferred conformations are *syn* and *anti*. *Syn* conformation is found in the Z-form of DNA, while *anti* conformation is the relative spatial orientation of the base and sugar found in most conformations of DNA³. In the illustration below, the preferred *anti*-conformation shows the purine ring is perpendicular to the furanose ring and projects away from the furanose ring, whereas in the *syn* conformation the purine ring projects over the furanose ring (Figure 3).



Nucleoside
(Adenosine)



Nucleotide
(Adenosine 5'-monophosphate)

Figure 1. Structure of nucleosides and nucleotides.

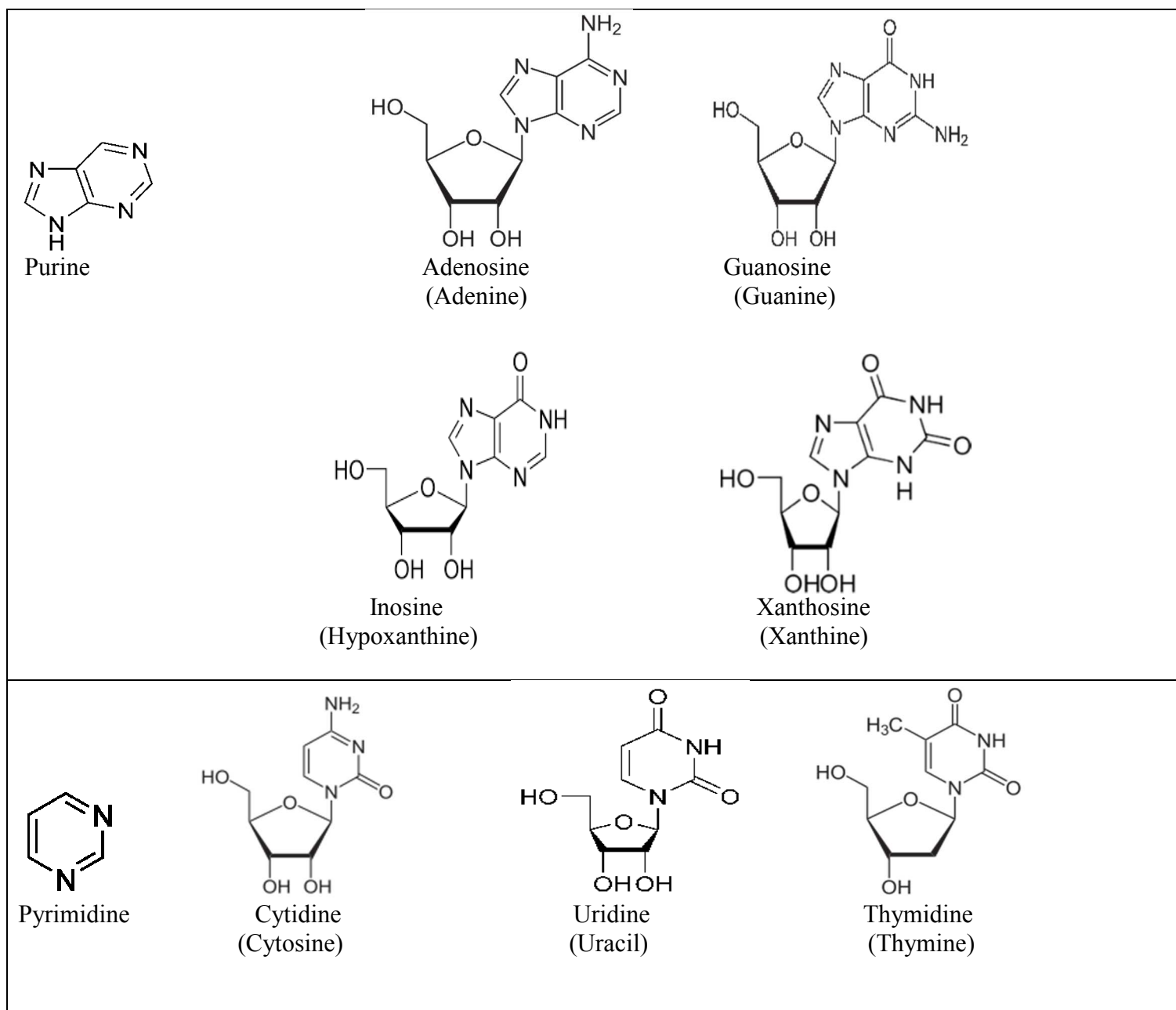


Figure 2. The common purine and pyrimidine nucleosides. Thymidine contains 2'-deoxyribose, while the other nucleosides contain ribose. The name of the nitrogenous base is in parentheses.

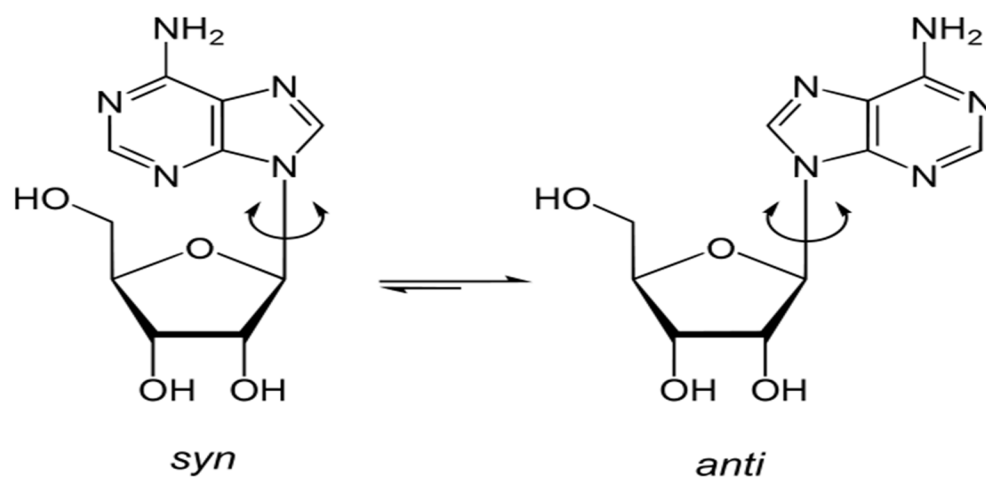


Figure 3. Structures of *syn* and *anti* purine nucleoside conformations. The figure shows the orientation of base to sugar around the glycosidic bond in purine nucleosides.

1. Purines and Pyrimidines

Purines are heterocyclic compounds that consist of a 6-membered and a 5-membered nitrogen-containing ring, fused together. Common purines are adenine, guanine, hypoxanthine and xanthine (Figure 2). Adenine is 6-amino purine and guanine is 2-amino-6-oxy purine. Hypoxanthine and xanthine are important intermediates in the synthesis and degradation of the purine nucleotides. Hypoxanthine is the base component of inosine, while xanthine is the base component of xanthosine.

Pyrimidine bases consist of a 6-membered ring with two nitrogens and four carbons. Common pyrimidines are cytosine, thymine, and uracil (Figure2). Cytosine is 2-oxy-4-amino pyrimidine. Thymine is 2, 4-dioxy-5-methyl pyrimidine. Uracil is 2, 4-dioxy pyrimidine. Uracil is similar to thymine but lacks the methyl group at C5.

2. Nucleoside Hydrolases

Nucleoside hydrolases are a group of enzymes that catalyze the hydrolysis of the β -N-glycosyl bond in nucleosides⁴. These enzymes are found in various organisms including protozoa, plants, bacteria, and insects among others^(5, 6, 7). The classification of the nucleoside hydrolases are based on the differences in their substrate specificities and the ability to hydrolyze both ribo- and deoxyribonucleosides. Based on their substrate specificities, nucleoside hydrolases are classified as: purine-specific (IAG-NH), nonspecific (IU-NH), pyrimidine specific (CU-NH), and 6-oxopurine specific (GI-NH)^(9, 10).

Parasitic protozoa such as *Leishmania major*, *Crithidia fasciculata* and *Trypanasoma brucei* lack a purine *de novo* biosynthetic pathway and therefore require extracellular purines for RNA and DNA synthesis^(8, 11). These purines are supplied by the salvage pathway of which the nucleoside hydrolases are a part. Nucleoside hydrolases of many protozoans have been cloned

and sequenced. Inosine-uridine nucleoside hydrolase (IU-NH) from the protozoan *C. fasciculata* was the first cloned and characterized nucleoside hydrolase of protozoa.^(11, 12) Several more nucleoside hydrolases have been cloned including IU-NH from the protozoan of *L. major*, a non-specific nucleoside hydrolase from *Leishmania donovani*, and a purine-specific nucleoside hydrolase from several trypanosomes such as *T. brucei* and *Trypanosoma vivax*^(8, 13).

The *Escherichia coli* genome contains genes for three ribonucleoside hydrolases, *ybek*, *yeik*, and *yaaf* enzymes also known as *rihA*, *rihB* and *rihC*¹⁴. In 2000, Petersen and Moller determined the substrate specificity of the three ribonucleoside hydrolases by transforming CN2573, a multiple mutant, with recombinant plasmids containing the structural genes of *rihA*, *rihB* and *rihC*. They measured the resulting hydrolytic activities with different nucleoside substrates. The results indicated that both *rihA* and *rihB* were pyrimidine specific and showed a preference for cytidine over uridine. On the other hand, *rihC* hydrolyzed both purine and pyrimidine ribonucleosides with decreasing activity in the order uridine > xanthosine > inosine > adenosine > cytidine > guanosine¹⁴.

3. Nucleoside Hydrolases from *Escherichia coli*

In developing countries, bacterial diseases remain a huge healthcare problem, and cause many internal or external infections of animals and humans³. *E. coli* is widely distributed in nature, and frequently the cause of infections of the urogenital tract and neonatal meningitis and diarrhea in infants¹⁵. Most *E.coli* cause no harm, but some strains can cause serious illness and even death. The most common symptoms of *E.coli* infections are stomach cramps, blood in stool, diarrhea and fever^(16, 17). People suffering from an *E. coli* infection usually recover within 7-10 days. The most recent deadly outbreak of *E. coli* infection occurred in Germany in May 2011,

where approximately 4000 people were infected by an *E. coli* strain, known as O104:H4, resulting in 50 deaths¹⁸.

In *E. coli*, many enzymes are involved in the recycling of purines and pyrimidines nucleosides. RihC hydrolyzes both purine and pyrimidine ribonucleosides⁵. For example, it hydrolyzes adenosine to yield adenine and ribose (Figure 4). Other studies show that rihC is similar to the IU-NH of *C. fasciculata* and shares interactions with substrate and amino acids at the active site¹⁹. However, many of the characteristics of the rihC enzyme are still unclear^(9, 19).

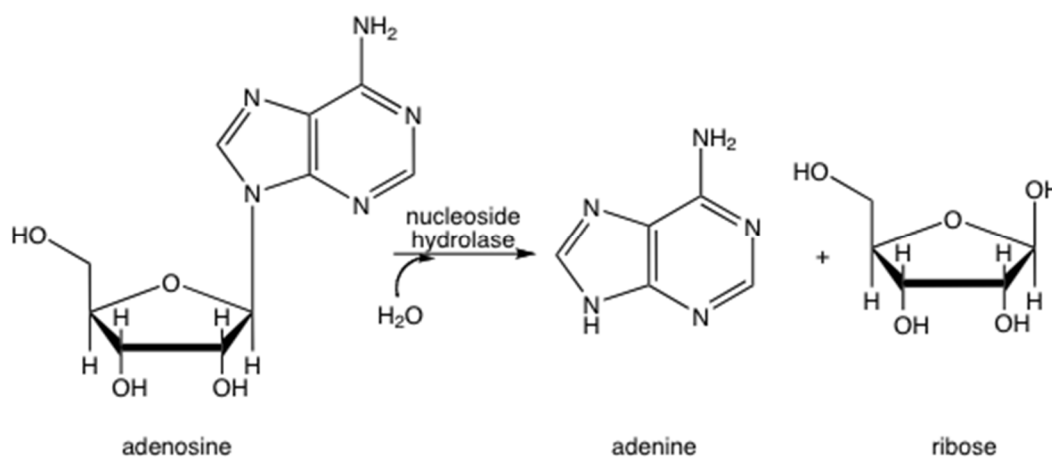


Figure 4: Hydrolysis of adenosine to adenine and ribose.

4. Structures Representative of Different Parasitic Groups of Nucleoside Hydrolase

The structural and functional comparison of a non-specific and a purine-specific nucleoside hydrolase will now be discussed. The crystal structure of the nonspecific IU-NH of *C. fasciculata* has been solved along with the purine nucleoside hydrolase IAG-NH of *T. vivax*¹⁵. Inosine-uridine nucleoside hydrolase has been crystallized as a homotetramer and inosine-adenine-guanosine nucleoside hydrolase (IAG-NH) as a homodimer (Figure 5a, b). The IU-NHs are tetramers and the subunit-subunit interfaces are formed mainly by β -strands and coils, with

the subunits pointing in a different relative orientation than they do in the IAG-NH^(15, 20). In architecture and topology, the subunits of IU-NH and IAG-NH are similar and consist of a single globular domain (Figure 5c, d). Two loops (loops I & II in Figure 5c, d) are positioned on each side of the active site. The active site is located near the C-terminus¹⁵.

Nucleoside hydrolases contain one deep narrow active site per subunit¹⁵. At the bottom of the active site, a calcium ion is tightly bound. Binding the nucleobase in *C. fasciculata* requires various amino acid residues including Phe167, Ile81, Tyr229, Tyr225 and His82. The enzyme substrate interactions in IU-NH of *C. fasciculata* show residues involved in hydrogen bonding to the three hydroxyl groups of the sugar. These residues include Asp10, Asp14, Asp15, Asn39 and Asp242 for the 2'- and 3'-hydroxyls; Asn160, Glu166, and Asn168 for the 5'-hydroxyl (Figure 6a, c). His241 has been proposed to be involved in the activation of the leaving group by protonating N7 of a purine base¹⁹. A mutant in which His241 was changed to alanine exhibited a 2000-fold reduction in activity with inosine, but maintained activity toward substrate *p*-nitrophenyl β -D-ribofuranoside, which is not activated by leaving group activation¹⁹. In *T. vivax*, the octacoordinated metal is chelated through a conserved network of interactions involving the side chain oxygens of Asp10, Asp15, and Asp261, the main chain carbonyl oxygen of Thr137 and three water molecules (Figure 6b, d)¹⁵. Residues interacting with the three hydroxyl groups of the substrate ribose included Asp14, and Asp261 for the 2'- and 3'-hydroxyl groups and Glu184 for the 5'-hydroxyl.

Amino acid sequence alignments of nucleoside hydrolases from a number of organisms highlight a recurring N-terminal DXDXXXDD motif as a fingerprint of nucleoside hydrolases²¹. Based on the sequence identity and conserved key amino acid residues, nucleoside hydrolases appear to fall into three distinct groups (Figure 7)²¹. Group I NHs contain a conserved histidine

that functions as a proton donor and is important for catalysis. The C-terminal region in this group contains the conserved histidine in the nucleobase-binding pocket. This group comprises pyrimidine specific (CU-NH) and nonspecific (IU-NH) nucleoside hydrolases. In Group II NH, histidine is replaced by tryptophan. This enzyme group contains IAG-NH. In group III, amino acids such as asparagine, cysteine, and proline occur in the catalytic site. This group includes IG-NHs. The aspartate cluster located in the N-terminal region is involved in binding the active site Ca^{2+} and water nucleophile. The aspartate cluster is conserved in all nucleoside hydrolase proteins ²¹. At the C and N termini, protein residues interacting with the calcium ion or ribose ring are highlighted (Figure 7) ²¹.

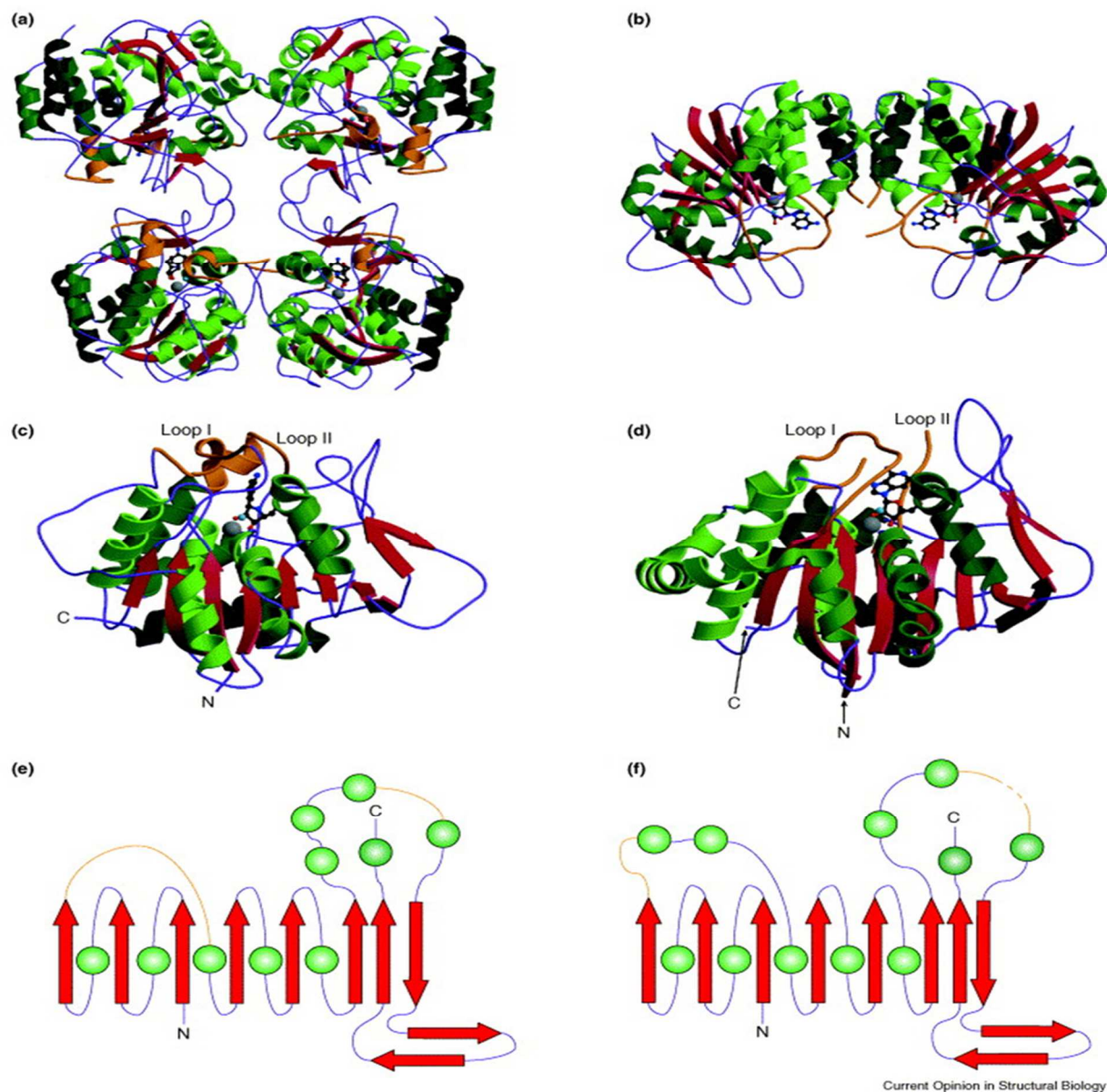


Figure 5. Distinct quaternary structures, tertiary structures, and topologies of *Crithidia fasciculata* IU--NH (a, c, e) and *Trypanosoma vivax* IAG-NH (b, d, f). Helices are shown in green and sheet strands are in red. The Ca^{2+} ion and the nucleophilic water molecule are in the active site pockets and represented as grey and blue spheres. In orange are two flexible loops in the vicinity of the active site. Reprinted from Versees, W; Steyaert, J. *Current Opinion in Structural Biology*. **2003**, 13, 731-738.

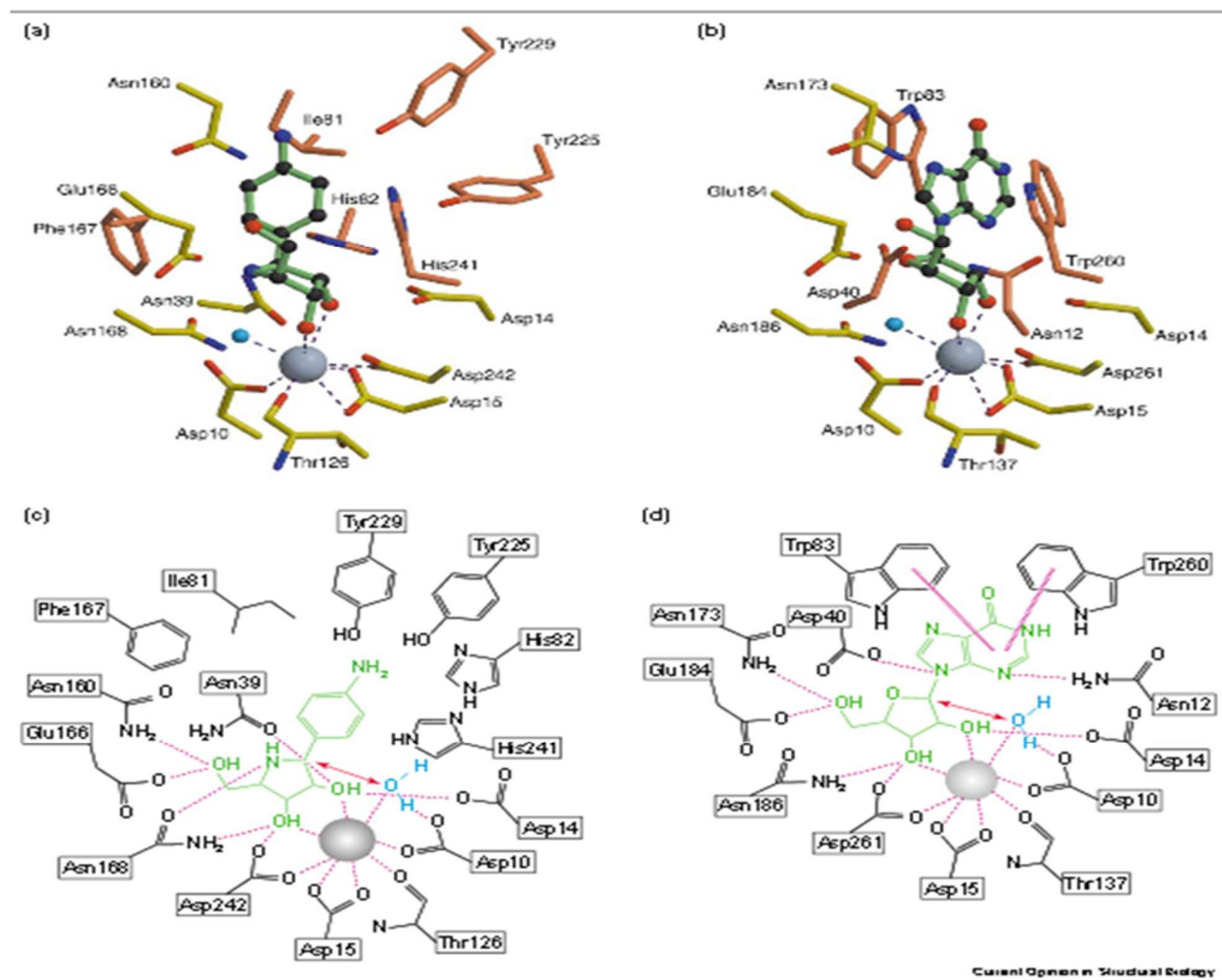


Figure 6. Comparison of the active sites of IU-NH (a, c) in complex with pAPIR and IAG-NH (b, d) in complex with inosine. The structural model of wild-type TvNH in complex with the natural substrate inosine was obtained by replacing 3-deaza-adenosine of the wild-type-3-deaza-adenosine complex (PDB code 1HP0) with inosine from the Asp10Ala IAG-NH inosine complex (PDB code 1KIC) upon superposition of both structures. The enzyme-bound ligands are shown in green. The Ca²⁺ ion and the nucleophilic water molecule are depicted as grey and blue spheres, respectively. In (a, b), the more conserved active site residues interacting with the Ca²⁺ ion and the ribose moiety are shown in yellow, whereas the residues of the nucleobase-binding pocket are shown in light brown (c, d). Schematic representation of the intermolecular interactions. Possible interactions are indicated by magenta dotted lines. The pink arrows indicate the nucleophile and the electrophilic center of the substitution reaction. The nucleobase in the TvNH–inosine complex is stacked between the side chains of Trp83 and Trp260 (d). Reprinted from Versees, W; Steyaert, J. *Current Opinion in Structural Biology*. **2003**, 13, 731-738.

N-terminal region

```

RihA -----MALPILLDCDPGHDDAIAIVLALASPE
LmNH -----MPRKIILDCDPGIDDAVAIFLAHGNPE
CfNH -----MPKKIILDCDPGLDDAVAILLAHGNPE
TvNH -----MAKNVVLDDHGNLDDFVAMVLLASNTE
Tbb1 -----MAKTVILDDHGNKDDFVAMILLLSNPK
Sagalactia -----MNKEKIIIDCDPGIDDLALMYAIQHPK
Aegypti -----KGIRRVIIDQGGGDDGWALLMMLMNEK
Tbb2 -----MVHRKLIIDTDCGGDDAIAIMLAMTQPD

```

C-terminal region

```

RihA TIVAELLDFLEHYHKDEKWFVVGAP-----HDPCTIAWLLKP
LmNH -----E-HDTYGKV-----HDPCAVAYV
CfNH RFMLEIMDYTKIYQSNRYMAAAAV-----HDPCAVAYVIDP
TvNH SILVGTMWAMCTHCELLRDGDGYA-----WDALTAAYVVDQ
Tbb1 SQMVGTMWAMSTHEEILRDGDAYYA-----WDALTAAYILEP
Sagalactiae SFIQKITKFYDFHWQYEHIIG-----NDPLAIAYFVNE
Aegypti KAIVVLNQVEEVIYANISNWQP-----CDMYAAAVLLNN
Tbb2 EFIEKLFQRLEAFTRIHDGTR-DTGDAEATQDVTCVVPD-----DAVAVLVAIRP

```

Figure 7. Amino acid sequence alignment for 8 selected putative NH proteins: RihA, the CU-specific NH from *E. coli*; CfNH, the IU-specific NH from *Crithidia fasciculata*; TvNH, the IAG-specific NH from *Trypanosoma vivax*; Tbb1, the IAG specific NH from *Trypanosoma brucei brucei*; *Sagalactiae*, the NH from *Streptococcus Agalactiae*; *A. aegypti*, the NH from *Aedes aegypti* and *Tbb2* the second NH from *Trypanosoma brucei brucei*. Top panel, the N-terminal region with the aspartate cluster highlighted in red. Bottom, the C-terminal region of the nucleobase binding pocket. The conserved histidine of group I NHs is highlighted in blue, the conserved tryptophan of group II in green and the residue at this position for group III in gray. The conserved aspartate residue is highlighted in red. Reprinted with permission from Giabbai, Degano. *Structure*. **2004**, *12*, 739-749.

5. Enzymes

Enzymes are biological molecules that act as biological catalysts. They are necessary for life whether animal, plant, bacteria. They play an important role in living organisms by catalyzing reactions, shuttling intermediate compounds along direct pathways and providing control over biological processes. They are highly specific in their catalysis, and they must bind with the substrate into the active site to carry out a reaction.

6. Enzymes Kinetic and Mechanism

Enzyme kinetics is the study of the rate of a chemical reaction catalyzed by enzymes. Enzyme kinetics were introduced in 1902 when Adrian Brown investigated the rate of hydrolysis of sucrose by the yeast enzyme. He proposed that the overall reaction was composed of two elementary reactions ²².

Mechanism:

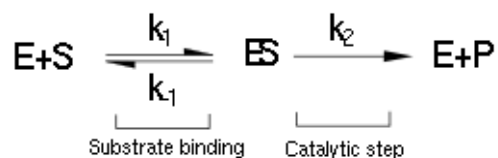


Figure 8. The enzyme- substrate complex (ES) provides the transitional state that facilitates a more rapid production of products.

In 1913, Lenor Michaelis and Maude Menten, building on the work of Victor Henri, made the assumption that the reversible step in the mechanism reaches equilibrium (Figure 8).

Therefore, rewriting the equilibrium expression for the reversible step and equating the ratio of the forward reaction to reverse rate constants and making substitutions yields the Michaelis-Menten equation shown in Figure 9 ²².

$$v = \frac{V_{\max} [S]}{K_M + [S]}$$

Figure 9. Michealis-Menten equation: V_{\max} is the rate of reaction at which all of the active sites of the enzyme are occupied by substrate. Michealis constant is a ratio of all rate constant involved and also represents the substrate concentration at which the reaction rate is half of maximal velocity. $[S]$ is the concentration of substrate binding to enzyme.

For many enzymes, plotting the rate of catalysis, the reaction velocity, (v) vs. the substrate concentration, $[S]$ results in a plot similar to that shown in Figure 10. Examining the plot, the reaction velocity seems to vary linearly with concentration when $[S]$ is small, but as concentration increases, the reaction velocity becomes independent of substrate concentration at large values. The Michaelis constant (K_m) is the substrate concentration at which the reaction rate is half of maximal velocity and is an important indicator of enzyme-substrate interactions. Another parameter from the Michaelis equation is the turnover number (k_{cat}). Turnover number is defined as the number of substrate molecules that can be converted to product in 1 second.

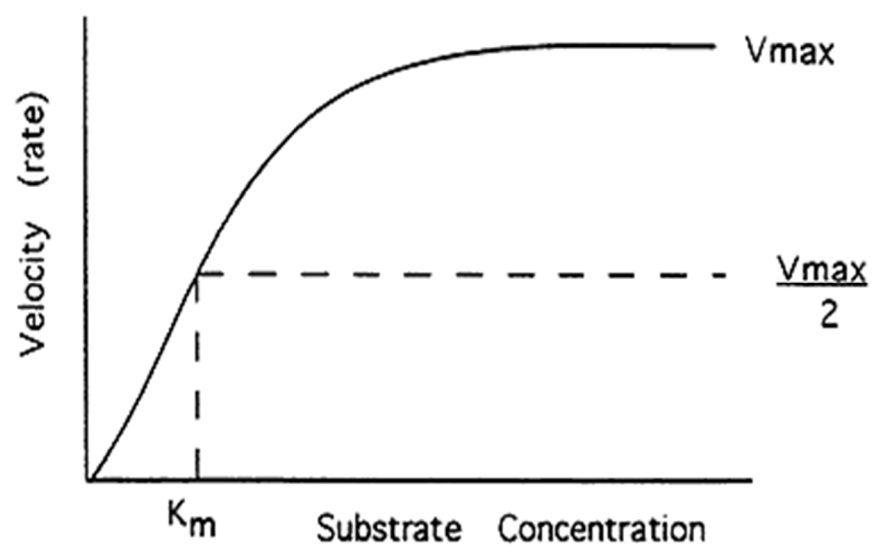


Figure 10. Michaelis-Menten kinetic. A plot of the reaction velocity (V_0) as a function of the substrate concentration $[S]$ for an enzyme that obeys Michaelis-Menten kinetics shows that the maximal velocity (V_{max}) is approached asymptotically. The Michaelis constant (K_m) is the substrate concentration at which the reaction rate is half of maximal velocity²².

7. Research Goal

The goal of this study is to determine the kinetic mechanism of *E.coli* RihC using inosine as a substrate, compare the kinetic data of the mutants with the wild type, and study the interactions between the substrate inosine and the mutants in the enzyme structure. To accomplish this goal, mutant enzymes were purified, kinetic constants determined, and molecular modeling techniques used to study the 3D structure of the enzyme.

CHAPTER II

MATERIALS AND METHODS

1. Materials and Reagents

The pET28b *rihC* mutants in *E. coli* were obtained from Brock Arivett. Laemmli sample buffer, 10x Tri/Glycine buffer, Protein Plus molecular marker, protein assay dye reagent, and protein standard were purchased from Bio-Rad. Pre-cast SDS-PAGE gels (4-12%) was purchased from Lonza. Pre-cast SDS-PAGE gels (12%), Gel Code Blue Safe stain, desalt spin columns, Slide-A-Lyzer G2 Dialysis Cassettes, and Pierce Silver Stain kit were obtained from Thermo-Scientific. Amicon Ultra-15 centrifugal filter units was purchased from Millipore.

2. Growth of Recombinant *E. coli* Cells

Growth of recombinant *E.coli* cells was performed by preparing 1L Luria broth (LB) medium containing 950 mL of deionized water, 10.0 g of tryptone, 5.0 g of yeast extract and 10.0 g of sodium chloride (NaCl). The solution was mixed until all the solids dissolved. The pH was adjusted to 7.0 with 1M sodium hydroxide. Deionized water was added to a final volume of 1 L. The solution was distributed into 2-25 mL Erlenmeyer flasks and 4- 250 mL flasks. The solutions were sterilized by autoclaving. Approximately 25 μ L of kanamycin and chloramphenicol (50 mg/mL) were added to each of the two 25 mL solutions. The 2 small flasks containing 25 mL solutions were inoculated using the *E.coli* cultures prepared by Brock Arivett. The solutions were incubated at 37°C and with shaking at 210 rpm overnight. The 25 mL solutions were used to inoculate the remaining 250 mL LB media. These were placed in the incubator at 37°C and 210 rpm. Four hours later, 2.5 mL of isopropyl- β -d-thiogalactopyranoside (IPTG) solution (1mg/mL) were added to each growth flask to initiate the expression of the recombinant protein and the flasks were returned in the incubator for overnight growth. The

cells were harvested by centrifugation at 10,000 xg for 45 minutes at 4°C. The cell pellets were resuspended in 10 mL of 50 mM sodium phosphate/300mM sodium chloride buffer pH 7.0. The cells were treated with 10 mg (1mg/mL) lysozyme in order to help break down the cell wall. The cells were incubated on ice for 30 minutes, and then sonicated 4 times for 15 seconds with a 2 minute recovery period. The disrupted cell resuspension was centrifuged for 30 minutes at 4000 xg at 4°C.

3. Purification of Enzyme

The six histidine residues added to the N terminus of the recombinant protein allowed an easy purification using nickel column affinity chromatography²³. The cleared lysate was loaded onto a Ni column (10 × 100) cm. Unbound proteins were washed from the column with 50 mM sodium phosphate, 300 mM NaCl, 10 mM imidazole buffer pH 7.2 wash buffer. The column was extensively washed with 200 mL wash buffer. Native elution buffer, pH 7.2 containing 50 mM sodium phosphate, 300 mM NaCl, and 100 mM imidazole was applied to the column and 15 mL fractions were collected. After collecting all the fractions, the absorbance of each fraction was determined at 280 nm using a Hitachi Model V-2900 UV-VIS spectrophotometer. The activity of each fraction was determined by reducing sugar assay. The fractions containing significant activity were pooled and concentrated to 5 mL. The concentrated eluate was dialyzed overnight against 10 mM Tris pH 7.0. The purified protein was stored at -4°C for further study. Approximately 2 mg of dithiothreitol was added to the protein solution to maintain activity. These purifications steps were applied to both wild type and mutants of rihC from *E.coli*.

4. Reducing Sugar Assay

Reducing sugar assay was performed to determine the activity of the enzyme eluted from the column. In order to test each fraction, the followings steps were applied: 1) a 1000 μ L reaction

mixture consisting of 1 mM nucleoside in 10 mM Tris pH 7.0 was added to the test tube; 2) 100 μ L from the chromatography fractions were added to the test tube; 3) the test tube was incubated at 32° C for 4 hours; 4) the reaction was stopped by the addition of 300 μ L copper reagent and 300 μ L neocuproine; 5) the test tube contents were mixed by vortex; and 6) placed in a boiling water bath for 7 minutes. The darker orange color indicated the presence of ribose. Absorbance was measured at 450 nm. A standard curve was used to determine the amount of ribose produced (Figure 11).

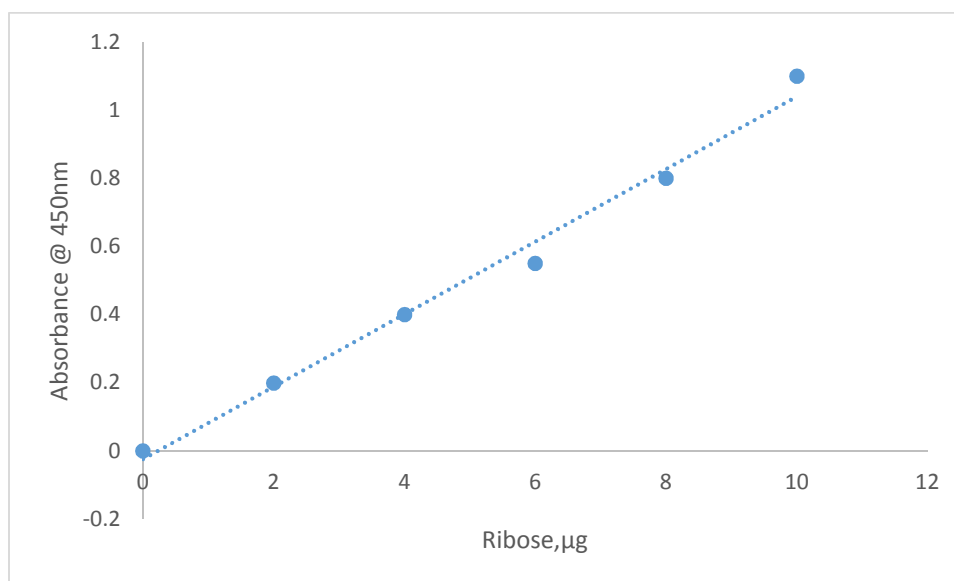


Figure 11. Standard curve for reducing sugar assay.

5. Protein Concentrations

Bio-Rad protein assay was used to measure total protein concentrations. A total of 800 μ L of deionized water/sample solution and 200 μ L dye reagent were added to a number of test tubes containing protein and vortexed. The solutions were incubated at room temperature for 5

minutes. Absorbance was measured at 595 nm. A standard, bovine serum albumin (1.44 mg/mL), was used to construct a calibration curve (Figure 12).

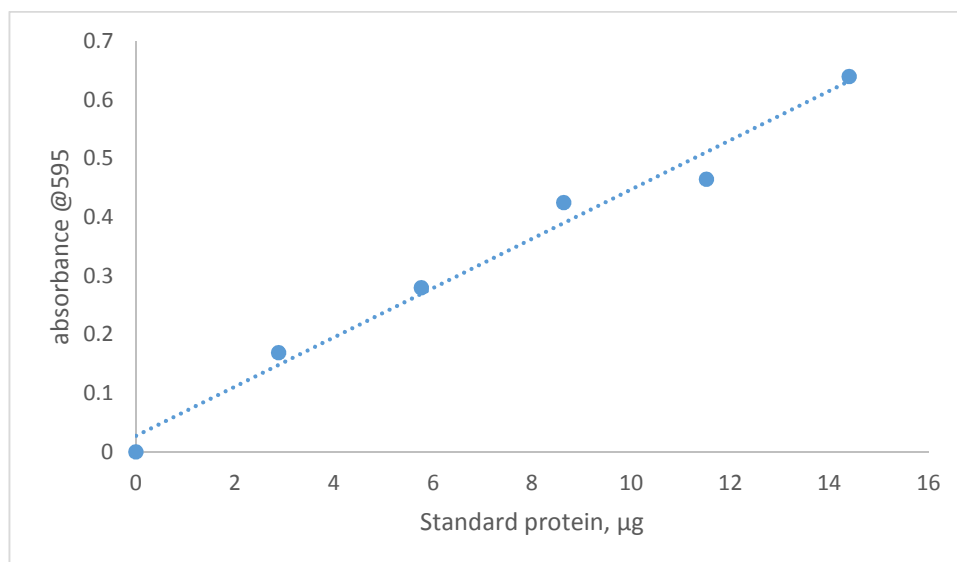


Figure 12: Standard calibration curve of protein absorbance 595 nm.

6. Determination of Enzyme Purity by SDS-PAGE Electrophoresis

Buffer solution for electrophoresis was prepared by a 1:10 dilution of 10x Tris/glycine SDS buffer (Bio-Rad) with water. Sample buffer was prepared by adding 50 μL 2-mercaptoethanol to 950 μL Laemmli sample buffer (Bio-Rad). Ten μL of enzyme sample were added to 10 μL of Laemmli buffer solution, centrifuged at 1000 rpm, and heated for 5 minutes at 95° C. The sample was then centrifuged for an additional 15 seconds. The sample was loaded onto a 4-12% SDS-PAGE gel along with Precision Plus Protein Unstained Marker. The gel was electrophoresed at a constant current of 30 mA for approximately 1 hour. After completion the gel was carefully removed from its plastic holders, washed with distilled water 3 times for 5 min each, and then covered with GelCode Blue Safe Protein Stain overnight. The Precision Plus Protein unstained molecular weight marker was used to construct the calibration curve. The molecular weight of

the protein sample was determined by comparison to the calibration curve.

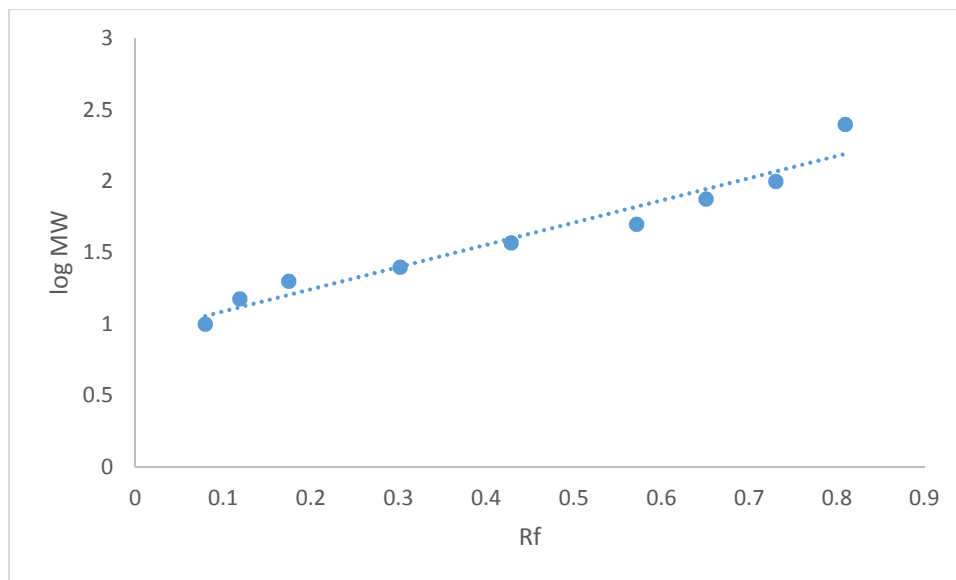


Figure 13. SDS-PAGE standard curve for Precision Plus Protein unstained molecular weight marker.

7. HPLC Analysis of Enzyme Activity

Enzyme activity was also determined by HPLC using 1 mL of reaction mixture containing different concentrations of inosine in 50 mM Tris buffer pH 7.0. The reaction was initiated by adding 10 μ L of enzyme to the inosine/Tris solution mixture.

The amounts of nucleoside bases were determined on a Dionex 3000 HPLC system. Separation of the nucleosides and bases was achieved using a Phenosphere ODS reverse phase column (150 \times 4.6 mm). The mobile phase was 10 mM ammonium phosphate pH 5.2/methanol in 98/2 ratio with flow rate of 0.600 mL/min. Each sample injection volume was 10 μ L. The nucleoside bases were detected at 254 nm. The nucleoside bases were identified by their

retention times. The amount of the enzyme activity produced was determined using a standard curve of the base concentration versus the reaction time.

8. Kinetic Activity

The kinetic parameters, Michaelis constant, K_m and the turnover number, k_{cat} were determined for various mutants of *E. coli rihC*. The turnover number for mutants D15, H233, L241, and F164 from *E. coli RihC* was calculated using the equation $k_{cat} = V_{max}/E_t$, where V_{max} is the rate of reaction in which all of the active sites of the enzyme are occupied by substrate and E_t is the concentration of enzyme in moles/L. These values were determined using the initial rate at different concentrations of inosine. The data were fitted by nonlinear regression analysis based on the Michaelis-Menten equation. The kinetic constant K_m was determined by steady-state analysis in which the velocity was measured in the presence of varying inosine concentrations. The inosine concentrations were 50 μ M, 100 μ M, 250 μ M, 500 μ M, 750 μ M, 1000 μ M, and 1880 μ M. The concentration of hypoxanthine produced was determined by HPLC as described earlier. The reaction velocity was calculated by dividing the concentration of hypoxanthine produced by the reaction time. The kinetic constant K_m for inosine nucleosidase was determined by nonlinear regression of the kinetic data to the Michaelis-Menten equation using Kaleidagraph software. All samples were analyzed in triplicate.

9. Structure Refinement

The structure of RihC of *E. coli* was modeled by sequence replacement using RihC *E. coli* nucleoside hydrolase in the search model on the CLC Drug Discovery workbench software. The protein sequence was imported by selecting sequence analysis on the toolbox menu. A number of available structures were found and ranked according to similarities in the sequences. RihA of *E. coli* Structure (PDB code 1YOE) was selected, imported and saved in the navigation area.

Protein structure was opened in 3D view. All solvent molecules, ligand and ions were removed. The residues D15, H233, F164, and L241 were identified, and labeled in the structure.

Binding and docking the substrate molecule to the enzyme were also performed using the CLC Drug Discovery workbench software. The substrate molecule was separately built using ChemDraw software (Figure 14), a 2D molecule sketcher software. The molecule was selected, and copied as Smiles options. The molecule was pasted to the molecule project and appeared in the ligands category in the project tree. A new category appeared in the project tree as the docking result. Previous to docking the molecule in the protein, the binding site was specified by double clicks on the “set up binding site” in the project setting. The dialog box opened and relevant molecules, residues, and interactions were automatically displayed in the 3D view. Structural interaction can be changed manually using the dialog box. Basic set ups such as protein preparation, ligand preparation, and targeted ligand docking were performed. Substrate molecule was docked into the protein and the structure was analyzed for interactions. This program allowed the docking of a substrate to the active site of the enzyme, and the determination of interactions with the hydroxyl groups in the ribose, and groups in the nitrogenous base.

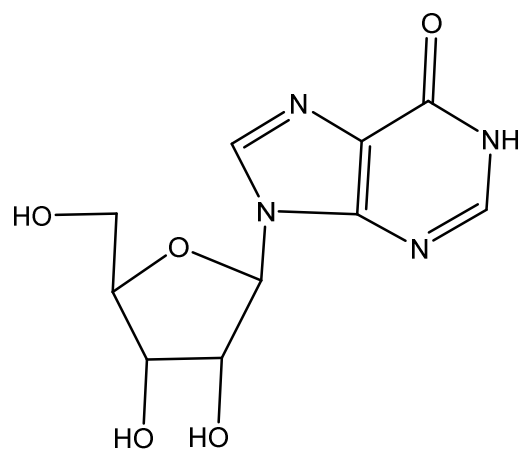


Figure 14. Two dimensional structure of inosine.

CHAPTER III

RESULTS AND DISCUSSIONS

Escherichia coli produces three types of nucleoside hydrolases, *rihA*, *rihB*, and *rihC*. RihA and rihB are pyrimidine-specific nucleoside hydrolases, while rihC is a nonspecific nucleoside hydrolase. Previous studies on inosine-uridine nucleoside hydrolase of *C. fasciculata* indicate that rihC enzyme belongs to the same class of nonspecific hydrolases²⁴. IU-NH is the most abundant nucleoside hydrolase in *Crithidia fasciculata*¹¹.

Alignments comparison of IU-NH from *Crithidia fasciculata* and the ribonucleoside hydrolases from *E. coli*, rihA, rihB, and rihC, determined that there are 69 conserved amino acid residues. RihC was more similar to rihA (59.8% similar, 43.7% identical) than rihB (54.8% similar, 36.6% identical) (Figure 15).

RihC of *E. coli* was cloned into a pET28 plasmid. The expression is under the control of the T7 RNA polymerase with a T7 promoter and is located upstream of the *Nde* I site between positions 270 and 286⁹. The enzyme was cloned with a His tag to facilitate purification. The plasmid was subjected to restriction digest and DNA sequencing to confirm the accuracy of the insert location⁹.

The wild type and mutants of rihC from *E. coli* were overexpressed by induction with 1mg/mL IPTG in LB solution. Cells were lysed by sonication and insoluble components removed by centrifugation. The soluble fraction was applied to a Ni agarose affinity chromatography column. Fractions containing significant activities were pooled and concentrated to a smaller volume (Figure 16). SDS-PAGE was used to assess the purity of the proteins. The protein concentrations were determined by Bio-Rad protein assay as described in the methods. Visual inspection of the stained gel showed that the enzymes were approximately 95% pure. The molecular weight was

calculated using a standard curve based on Plus Protein unstained standard (Figure 13). The molecular weight of the proteins was determined to be 33 kDa (Figures 17 and 18). The calculated molecular weight based on amino acid sequence is 32.57 kDa.

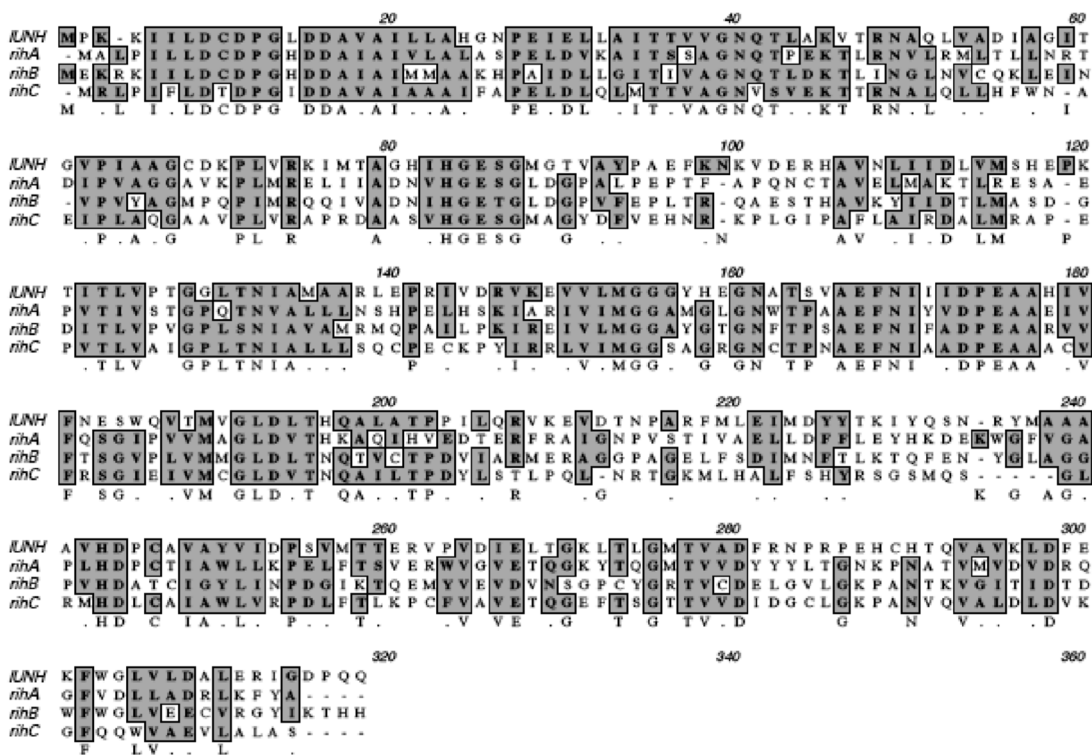


Figure 15. ClustalW comparison of *Crithidia fasciculata* and *E. coli* nucleoside hydrolases. Alignments of IU-NH from *C. fasciculata* and three nucleoside hydrolases from *E. coli*; RihA, RihB, and RihC, are shown. Common residues are noted in grey and the consensus sequence is shown on the last line. Reprinted with permission from Brock Arivett, M.S. thesis, Middle Tennessee State University.

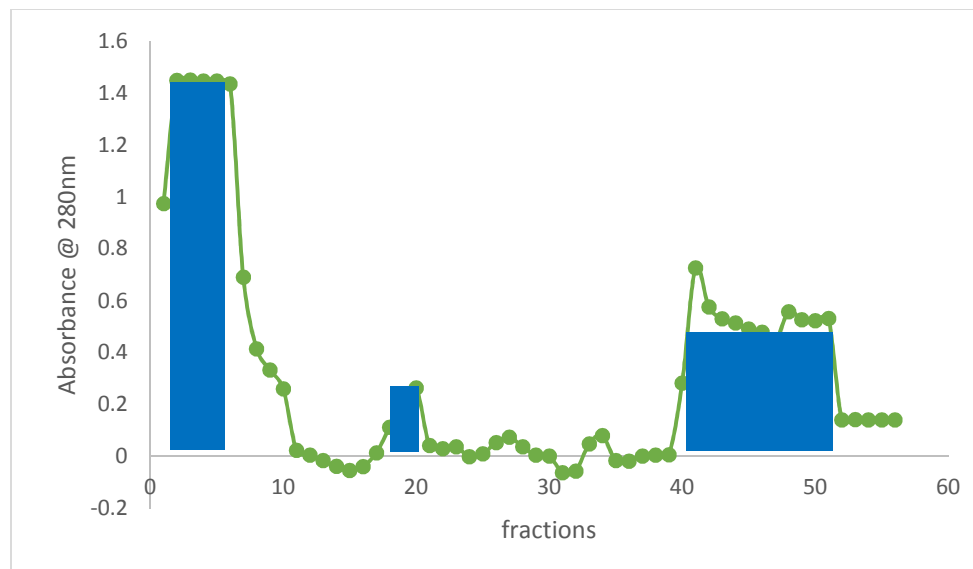


Figure 16. Mutant 233 elution profile after passage through a Ni agarose column. The green line is the absorbance of the H233 protein. Fractions selected on the basis of significant UV absorbance are marked in blue. Elution profiles for the other mutants and the wild type were similar.

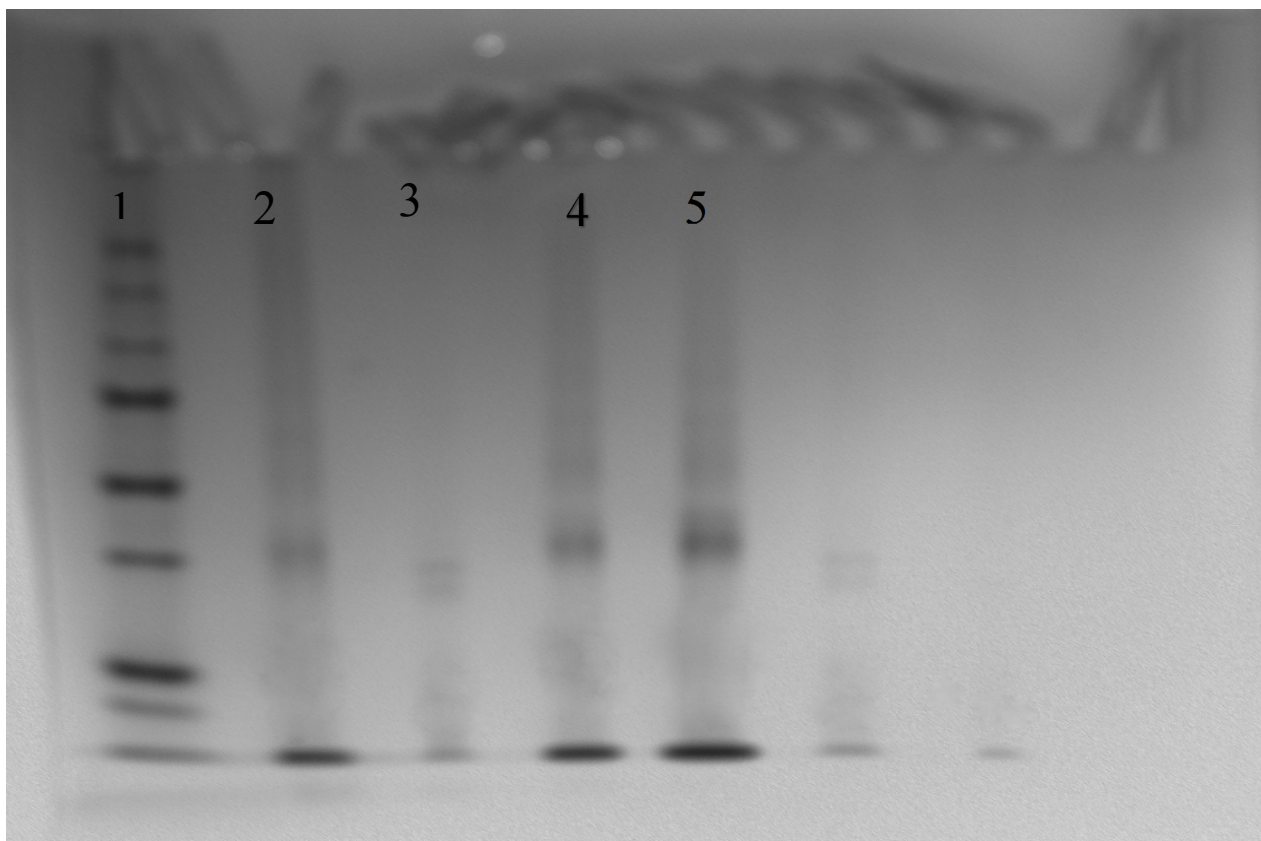


Figure 17. Coomassie blue staining of purified wild type and mutants of rihC from *E.coli*. Purified proteins were separated by 12% SDS-PAGE. The lanes were loaded as follows: 1) unstained protein standard; 2) wild type; 3) His233; 4) Leu241; 5) Phe164.

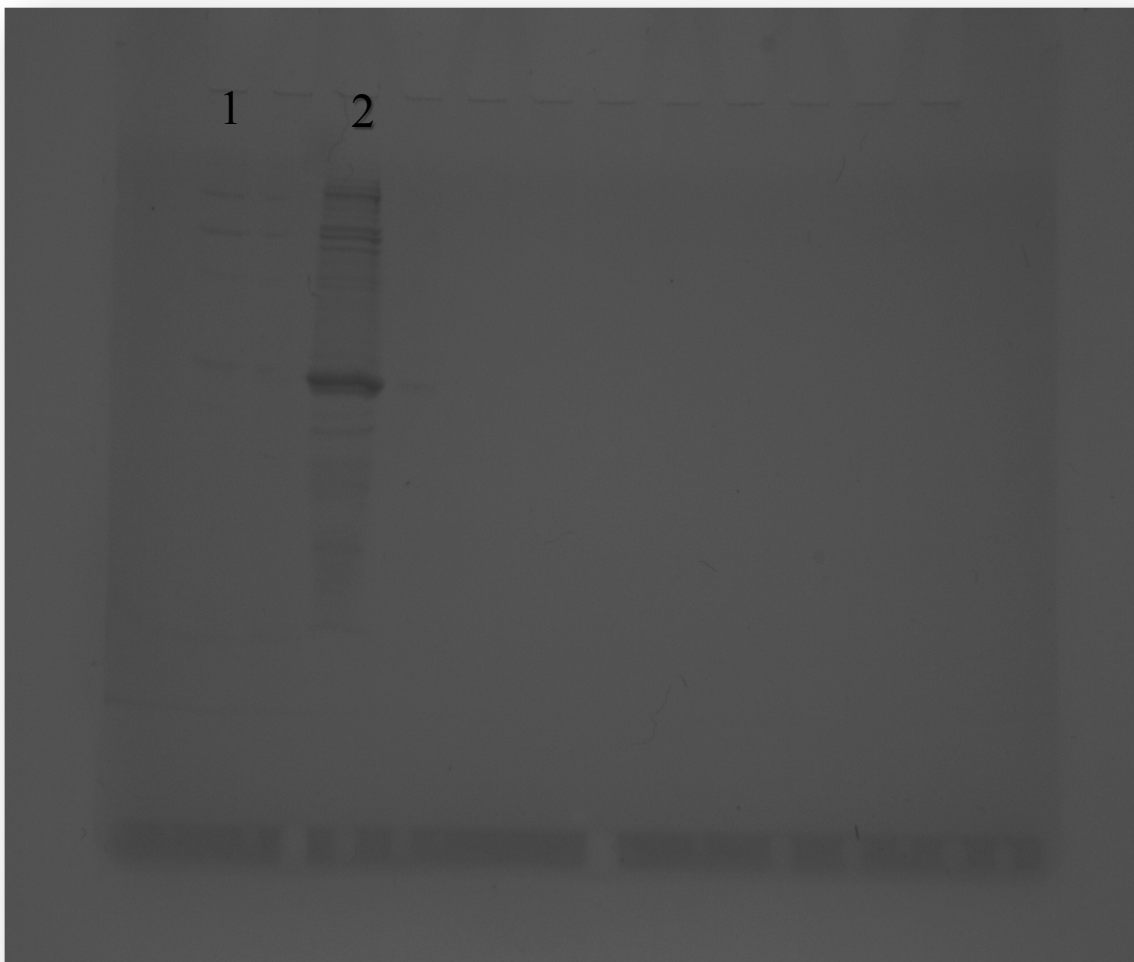


Figure 18. Coomassie blue staining of purified mutant 15 separated by 4-12% SDS-PAGE. Lane 1 is the unstained protein standard. Lane 2 is the Mutant D15.

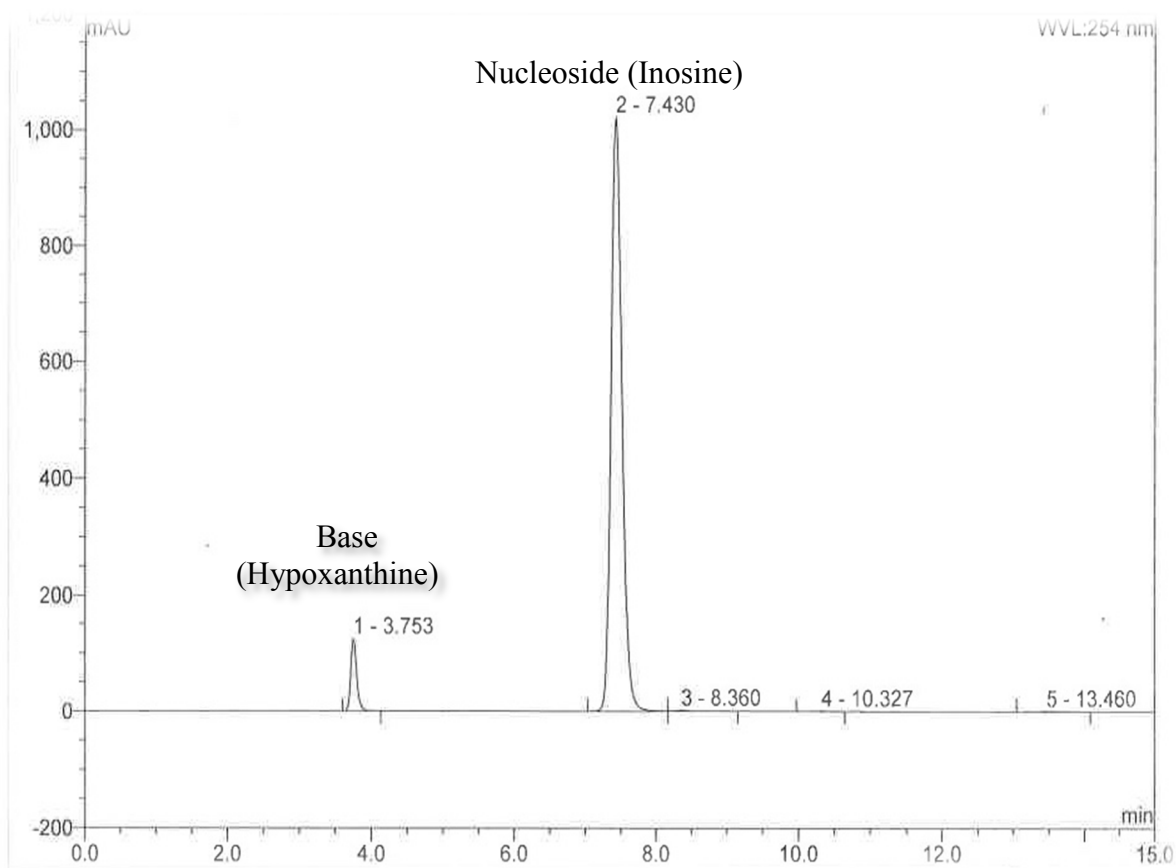
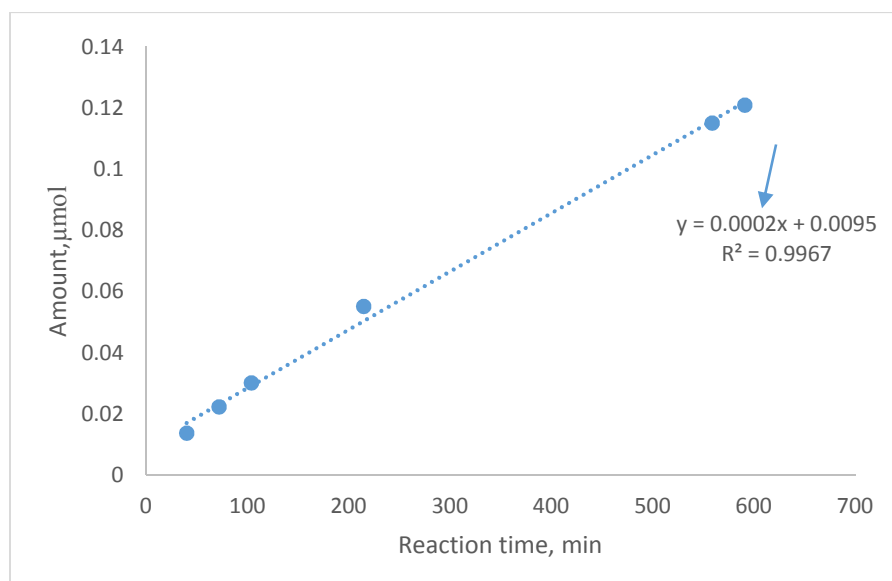


Figure 19. Typical protein HPLC chromatogram of wild type enzyme. The figure shows the separation of the base (hypoxanthine) from the nucleoside (inosine).

Table 1. Typical activity data of wild type

Reaction time (min)	% of hypoxanthine	Conc, μM	Amount, μmol
40	0.69	13.8	0.0138
72	1.12	22.4	0.0224
104	1.51	30.2	0.0302
215	2.76	55.2	0.0552
559	5.76	115.2	0.1152
591	6.05	121	0.121

**Figure 20.** Typical activity profile of wild type enzyme as a function of reaction time. The slope indicated by the arrow is the activity in $\mu\text{mol}/\text{min}$.

The effect of a mutation on the mechanism of rihC was determined by comparison of the kinetic parameters of the mutants to that of the wild type. Based on alignment with the sequence from IU-NH from *C. fasciculata*, four amino acids were chosen for mutation. These residues were D15, F164, H233, and L241. All of these residues were converted to alanines (Table 2).

As a first analysis, the specific activity of each mutant was compared to the specific activity of the wild type enzyme (Table 3). The wild type and all the mutants were active. Comparing the specific activity of wild type IU-NH from *E. coli* to mutants in which residues F164 and L241 were changed to alanines showed negligible effect on activity. Mutating residue 15 from an aspartate to an alanine resulted in an approximately 10-fold increase in activity. Of particular interest is the activity shown by the enzyme in which His233 is changed into an alanine. In *C. fasciculata*, a change in this residue resulted in an almost inactive enzyme⁹. In RihC from *E. coli*, the specific activity of the mutant was only lower than the wild type by a factor of 10. Contrary to expectations, His233 retained significant activity with inosine.

The Michaelis constant and k_{cat} of the wild type enzyme were determined by non-linear regression fitting of kinetic data to the Michaelis-Menten equation. RihC mutants from *E. coli* were also analyzed to determine their K_m and k_{cat} . To carry out this analysis, the activity of each enzyme was determined at different concentrations of inosine. The kinetic constants determined for each mutant using inosine as the substrate are shown in Table 4 and Figures 21-24. These values were compared with the wild type from recently published values to confirm the effect of various mutations on rihC from *E. coli*. The K_m and k_{cat} for the wild type were $422 \pm 225 \mu\text{M}$ and $4.31 \pm 0.22 \text{ s}^{-1}$ respectively^(9, 19). Residues F164, H233, and L241 show smaller k_{cat} values compared to the wild type (Table 4). The D15 mutant exhibited a higher value of k_{cat} . The K_m for these enzymes are similar to each other. D15 is the mutant which shows a 10-fold increase in

k_{cat}/K_m for inosine. The data are consistent with the specific activity obtained. In contrast the IU-NH from *C. fasciculata*, and IU-NH from *L. major* previously reported have a 95-fold and a 300-fold decrease respectively, while IU-NH from *E. coli* showed a less than 10-fold decrease in k_{cat}/K_m . Our data indicate that changes in the residues causes only minor changes in the catalytic properties of recombinant rihC of *E. coli*⁹.

Table 2. Amino acid changes and their role in rihC.

Original Amino Acids	New Amino Acids	Role in Enzyme
Aspartic acid (D) 15	Alanine	Stabilize the transition state
Phenylalanine (F) 164	Alanine	Binding substrate
Histidine (H) 233	Alanine	Proton donor
Leucine (L) 241	Alanine	Binding substrate

Table 3. Specific activities of mutants with inosine as substrate used in this study.

Mutants	Specific Activity, $\mu\text{mol}/\text{min}$ Inosine as substrate
Wild Type	6.09×10^{-5}
H233	8.5506×10^{-6}
L241	3.06×10^{-5}
F164	4.82×10^{-5}
D15	7.79×10^{-4}

Table 4. Kinetic parameters for wild type, and mutants D15, F164, L241, and H233 with inosine.

Mutants	K_m (μm)	k_{cat} (s^{-1})	k_{cat}/K_m ($\text{M}^{-1}\text{S}^{-1}$)
Wild type	$422 \pm 225^{(9)}$	$4.31 \pm 0.22^{(9)}$	1.02×10^4
F164	155 ± 30.0	2.24 ± 0.12	1.44×10^4
L241	161 ± 36.6	0.99 ± 0.06	6.1×10^3
D15	695 ± 190	145 ± 17.0	2.1×10^5
H233	554 ± 525	5.3 ± 2.3	9.5×10^3

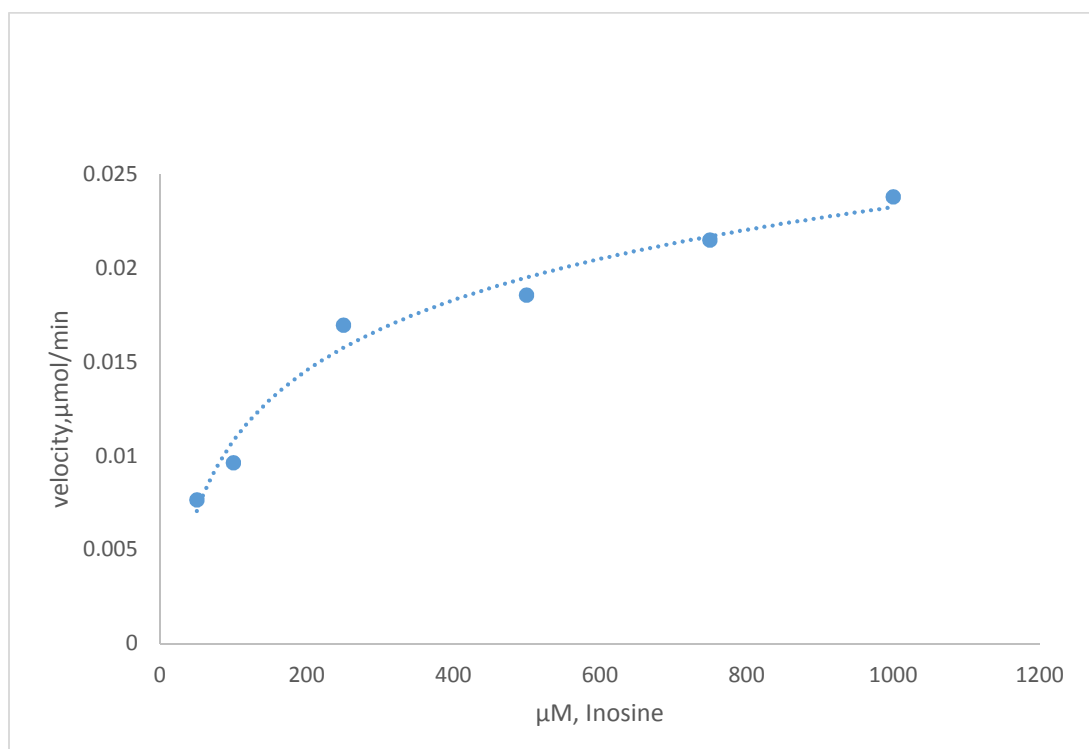


Figure 21. Kinetic analysis of inosine nucleoside hydrolase (rihC) of Mutant L241 (average of 3 trials). The substrate inosine concentrations used were 50, 100, 250, 500, 750, and 1000 μM .

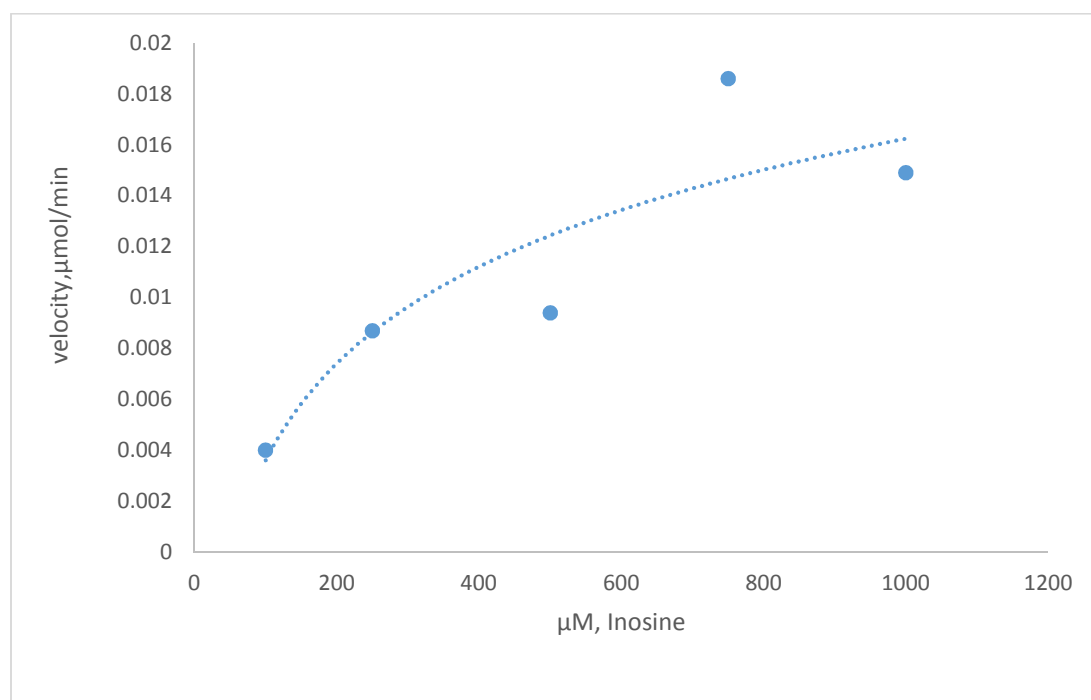


Figure 22. Kinetic analysis of inosine nucleoside hydrolase (rihC) of Mutant H233. The inosine concentrations used were 100, 250, 500, 750, and 1000 μM .

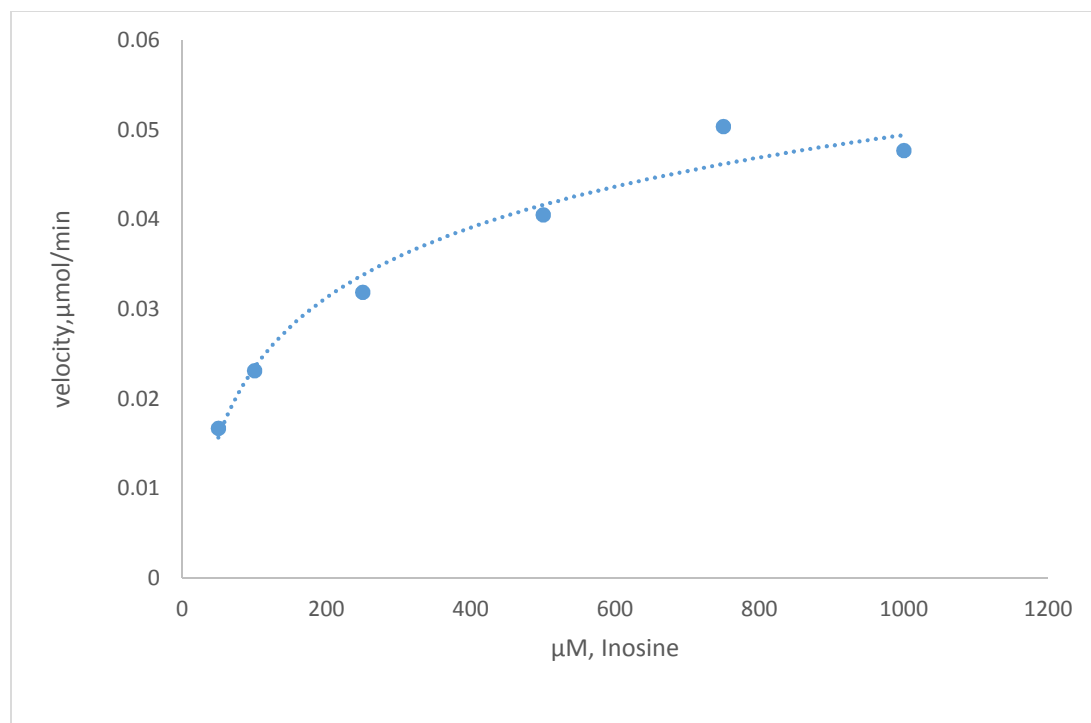


Figure 23. Kinetic analysis of inosine nucleoside hydrolase (rihC) of Mutant F164 (average trials). The inosine concentrations used were 50,100, 250, 500, 750, and 1000 μM .

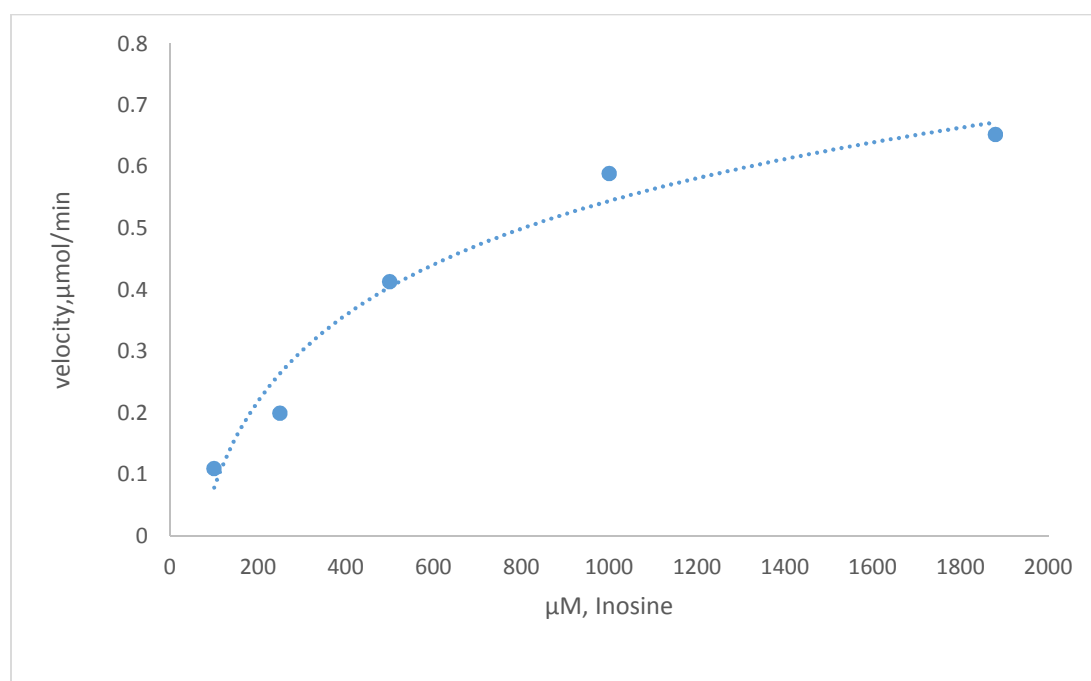


Figure 24. Kinetic analysis of inosine nucleoside hydrolase (rihC) of Mutant D15. The inosine concentrations used were 100, 250, 500, 1000, and 1880 μM .

Since no crystal structure is available for rihC enzyme, a 3D model was constructed using the structure of IU-NH from *C. fasciculata* as a template. First, the modeling of the structure was done to see if the three dimensional structure of rihC is similar to the IU-NH. Second, the substrate was docked to the active site of the enzyme. Third, hydrogen bonding patterns were determined to study the interactions between the substrate and the residues.

A structural comparison of inosine-uridine nucleoside hydrolase, the archetype nucleoside hydrolase of *C. fasciculata* (PDB 1MAS) and ribonucleoside hydrolase (RihC) of *E. coli* (PDB code 1YOE) were performed. Both enzymes were aligned using the CLC Drug Discovery Workbench program (Figure 25). The alignment comparison determined that IU-NH and RihC of *E. coli* (Figure 25) have 37% sequence identities (identical amino acids), 52% sequence similarities and 3% gaps. The sequence alignment of these proteins demonstrated that almost all the residues of interest are conserved in both RihC and IU-NH enzymes, aspartic acid (D) 15, phenylalanine (F) 164, histidine (H) 233, and leucine (L) 241. D15, F164, and H233 are identical in both proteins while L241 in rihC of *E. coli* is a valine in IU-NH of *C. fasciculata*.



Figure 25. Sequence alignment comparison of IU-NH from *Crithidia fasciculata* and RihC of *E.coli*. Dashes indicate missing sequence. Figure was generated from CLC Drug Discovery Workbench program.

The docking studies of RihC of *E.coli* were carried out to define the binding pocket, substrate interactions and enzyme specificities. The substrate inosine was docked into the active site of the enzyme to help understand the role of residues. The positions of residues D15, H233, L241, and F164 were analyzed (Figures 27 and 28). Residues in the catalytic site were connected to the inosine substrate by hydrogen bonding. Residue H233 positioned in the active site of the enzyme was hydrogen bonded to the substrate nitrogen at position 3 of hypoxanthine (28 and 30). According to Arivett and Farone, residue His233 has been proposed to protonate N7 of the hypoxanthine leaving group⁹. The side chain F164 pointed away from the active site. Residues D15 and L241 were too far away to interact with substrate. RihC from *E.coli* has previously been shown to be unable to catalyze the hydrolysis of substrates lacking 2'- and 3' hydroxyls while showing a 500-fold reduction in activity toward erythrouridine¹¹. Additional residues Asp14, Asp234, and Asn39 compose the active site. Asp14 and Asp234 show interactions with the 5' hydroxyl group, and Asn39 shows interaction with the 3' hydroxyl group.

The structure of IU-NH of *C. fasciculata* has been extensively studied¹⁹. The existing 3D structure for IU-NH of *C. fasciculata* bound with inosine was compared to RihC of *E. coli* in an attempt to understand the interactions between the substrate and the active site of the enzyme (Figures 29 and 31). When the crystal structure of IU-NH of *C. fasciculata* was analyzed His241 was positioned in the active site of the enzyme to interact with N7 of hypoxanthine (Figure 29). Additional residues in the active site include Asp15 and Asp10 which interact with 5' hydroxyl group, Asn168 interacts with 3' hydroxyl group, and Glu166 interacts with 2' hydroxyl group. These residues are hydrogen bonded with the substrate.

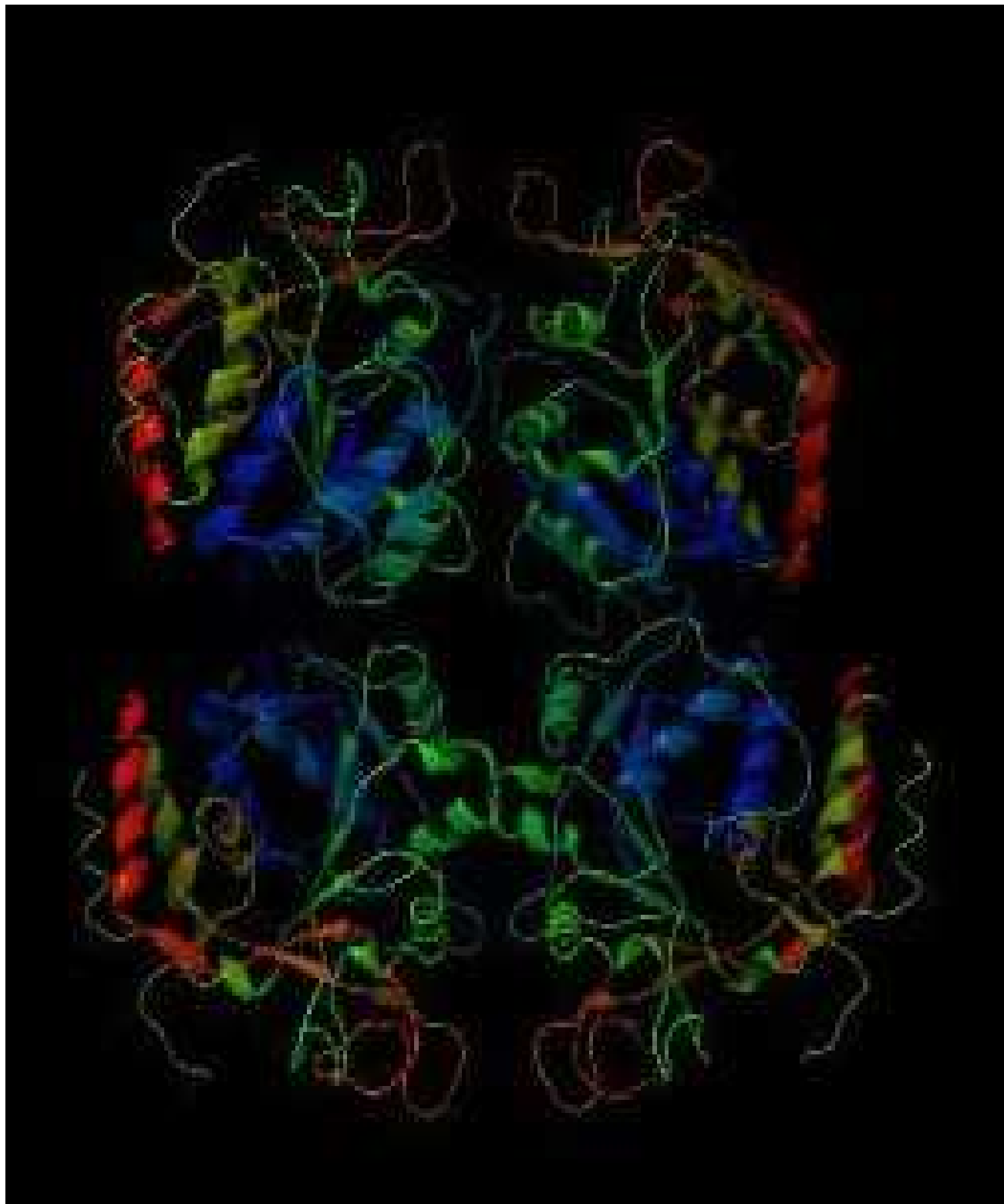


Figure 26. Tetramer structure of *E. coli* RihC. The proteins were modeled using CLC Drug Discovery Workbench program, using rihA of *E. coli* (PDB code 1YOE).

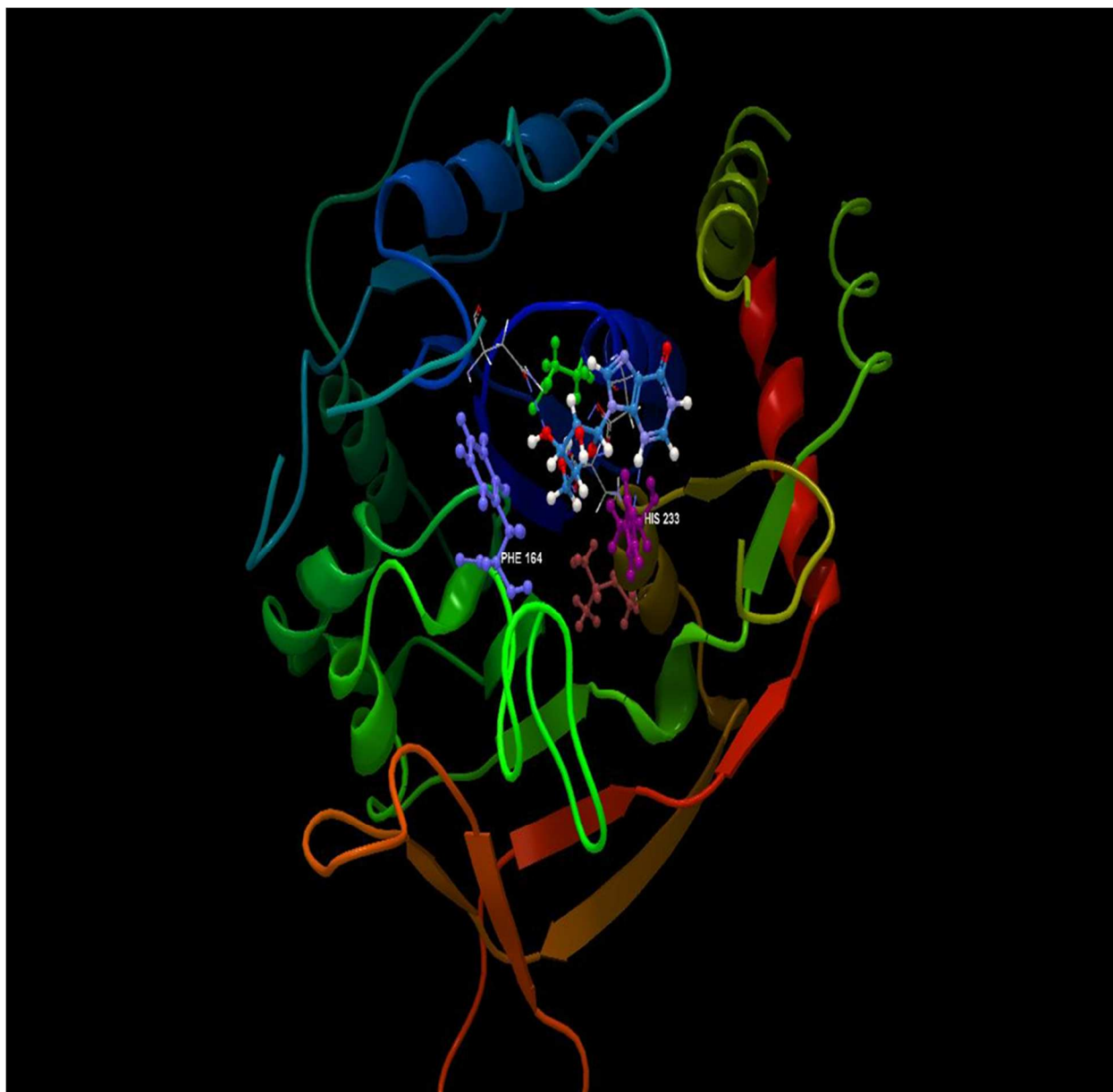


Figure 27. 3D Structure of RihC of *E.coli* monomer bound to inosine. Residues are represented as ball-and-stick model. Residues are indicated by different colors Asp15 green, His233 purple, Phe164 blue, and Leu241 pink. Hydrogen bonding is shown as dashed lines. Figure was generated with the CLC Drug Discovery Workbench program.

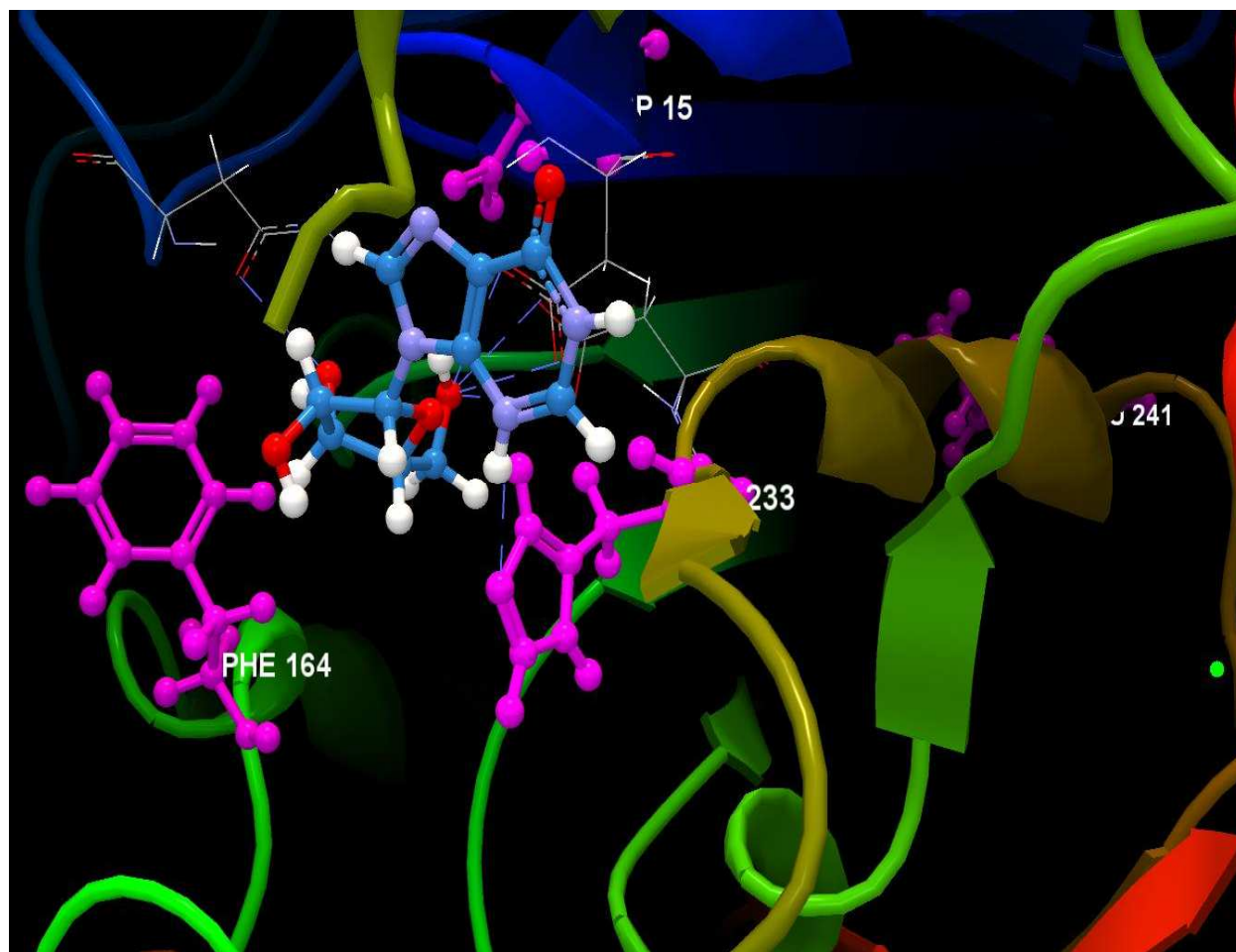


Figure 28. 3D Structure of RihC from *E.coli*. This figure shows residue interactions in the active site. Residues are in pink ball and stick. Molecule in the middle is inosine. Hydrogen bonds are represented as dashed lines.

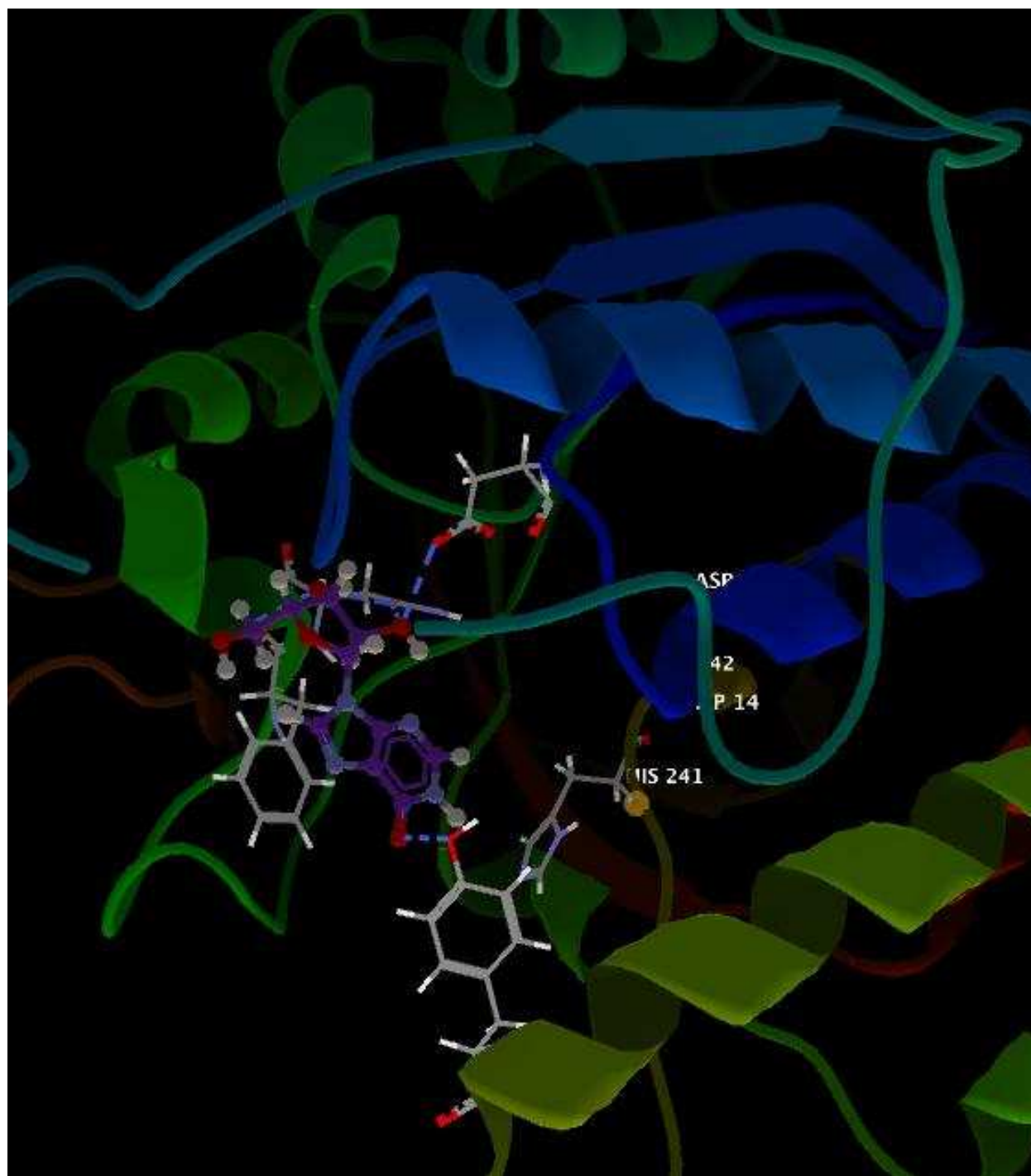
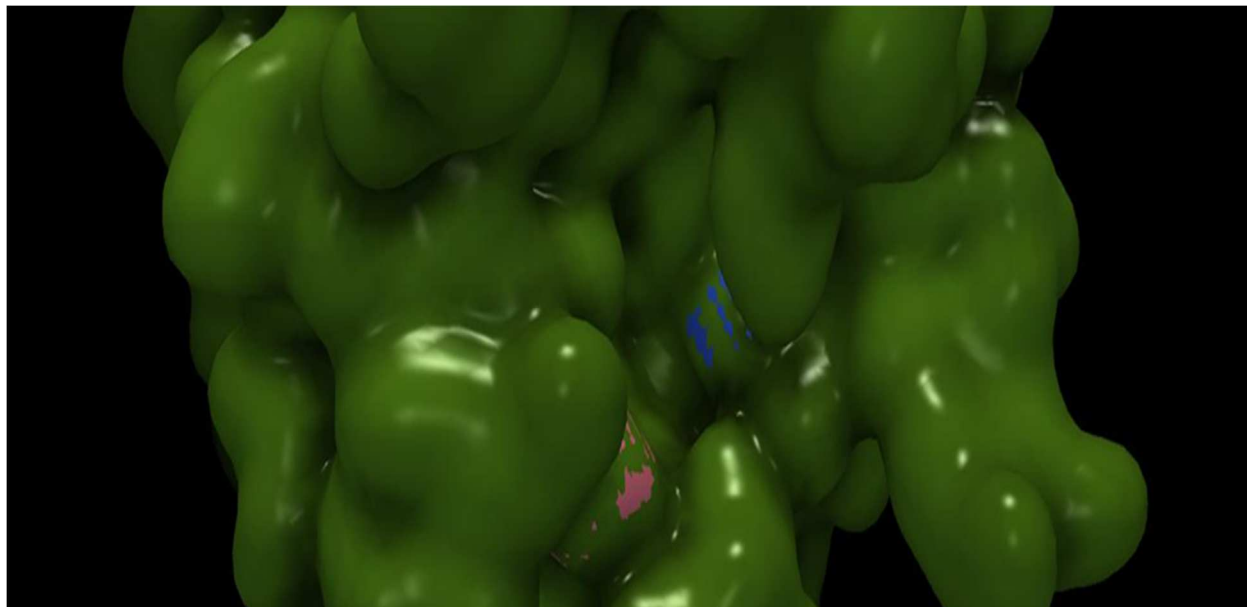


Figure 29. Crystal structure of IU-NH of *Crithidia fasciculata* bound with substrate inosine. His 241 is positioned to donate a proton to N7 of hypoxanthine.

a.



b.

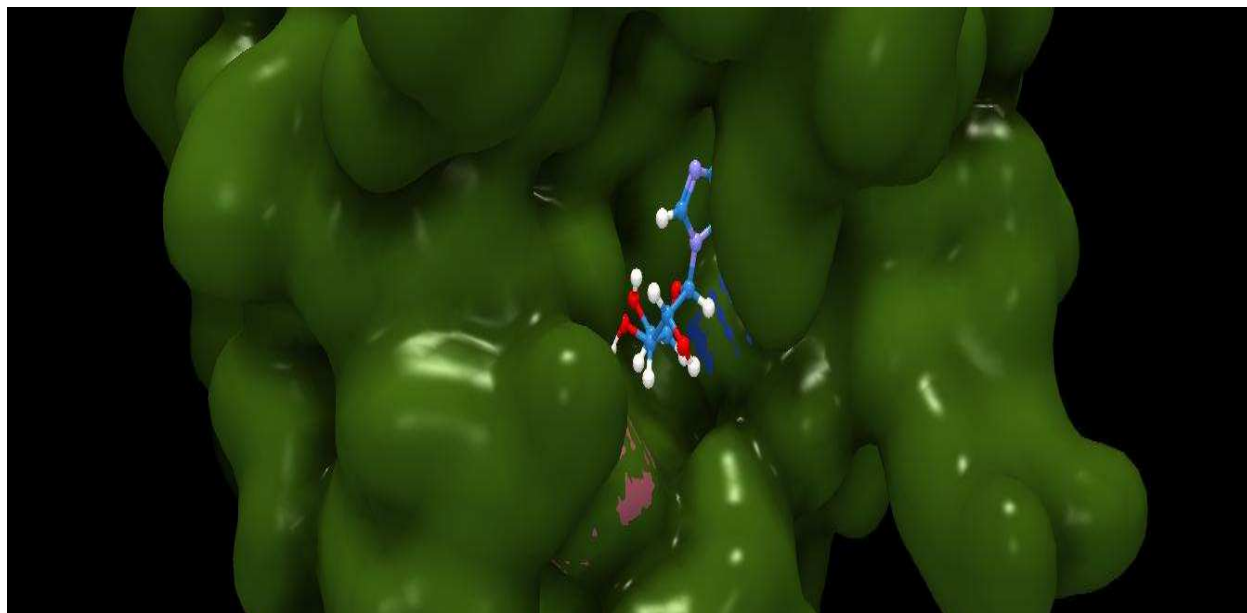


Figure 30. Molecular surface of RihC of *E.coli*. a) Structure of enzyme without substrate; b) Structure of enzyme with inosine bound in active site. His233 is shown in blue, while Phe164 is shown in pink.

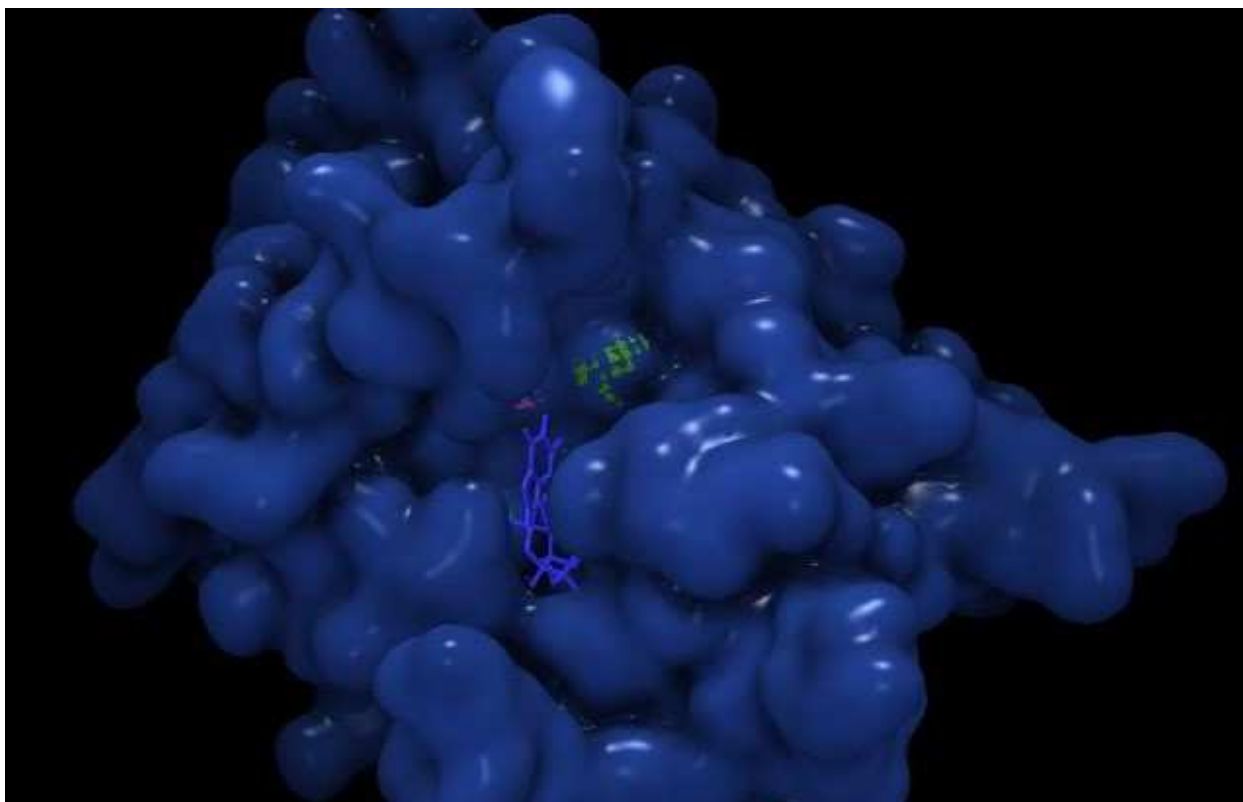


Figure 31. Molecular surface of IU-NH of *C. fasciculata*. Structure of enzyme with inosine bound in the active site. His 241 is shown in green, while Asp 14 is shown in pink.

CHAPTER IV

CONCLUSION

Ribonucleoside hydrolase (RihC) from *E.coli* is classified as a non-specific nucleoside hydrolase which is capable of hydrolyzing both purine and pyrimidines. RihC from *E. coli* and IU-NH from *C. fasciculata* have been proposed to share many features and functions¹⁹. RihC enzyme exists as a tetramer with 4 identical subunits⁴. Residues D15, H233, F164, and L241 were mutated to alanines. The mutant proteins were analyzed for size on SDS-PAGE. The molecular weight was 33 kDa consistent with the calculated molecular weight 32.57 kDa from the amino acid sequence. Kinetic studies of mutants H233, L241, F164, and D15 were used to establish the catalytic properties (k_{cat} and K_m) and compared to the wild type. Based on their kinetic parameters, these proteins did not show much difference compared to the wild type. Only mutant His233 showed a 10-fold reduction in activity. Therefore, the mutations did not significantly affect the enzyme.

To support the kinetic data, the 3D structure for the enzyme was built using CLC drug Discovery Design Workbench Program. RihC of *E.coli* and IU-NH *C. fasciculata* sequences were aligned. After docking the substrate in the active site of the enzyme, the number and position of residues involved in the active site were analyzed. The interactions between the substrate inosine and the enzyme in the catalytic site were hydrogen bonds. The His233 residue in the active site H bonded to N3 of the substrate rather than N7. F164 pointed away from the active site. D15 and L241 were positioned well away from the active site of the enzyme. None of the residues in this study is positioned for hydrogen protonation of N7.

Since detailed enzyme mechanism of rihC from *E.coli* has not yet been reported, more studies need to be done to support this work, including an analysis of mutated protein by mass

spectrometry in order to confirm the mutation of these amino acids. Additional residues can also be mutated, and their interactions studied in the reaction catalyzed by the enzyme.

REFERENCES

1. Muzzolini L., Versées W., Tornaghi P., Van Holsbeke E., Steyaert J., Degano M. **2006**. New insights into the mechanism of nucleoside hydrolases from the crystal structure of the *Escherichia coli* YbeK protein bound to the reaction product. *Biochemistry* 45(3): 773-82.
2. Lodish H., Berk A, Zipursky SL, et al. **2000**. The three roles of RNA in protein synthesis. *Molecular Cell Biology*. 4th edition. New York: W. H. Freeman. Section 4.4.
3. Qadri F., Svennerholm, A.-M., Faruque, A. S. G., & Sack, R. B. **2005**. Enterotoxigenic *Escherichia coli* in developing countries: Epidemiology, microbiology, clinical features, treatment, and prevention. *Clinical Microbiology Reviews*, 18(3):465–483.
4. Marston. F. A. **1986**. The purification of eukaryotic polypeptides synthesized in *Escherichia coli*. Protein Biochemistry Department, Celltech Ltd., 244-250
5. Ogawa J., Takeda S, Xie S.-X., Hatanaka H., Ashikari T., Amachi T., Shimizu S. **2001**. Purification, characterisation, and gene cloning of purine nucleosidase from *Ochrobactrum anthropic*. *Appl. Environ Microbiol.*, 67:1783–1787
6. Kline P. C., Schram V. L. **1993**. Purine nucleoside phosphorylase. Catalytic mechanism and transition-state analysis of the arsenolysis reaction. *Biochemistry*, 32: 13212–13219.
7. Cui L., Rajasekariah G.R., Martin S.K. **2001**. A nonspecific nucleoside hydrolase from *Leishmania donovani*: implications for purine salvage by the parasite?. *Gene*, 280: 153–162
8. Shi, W., Schramm V. L., and Almo S. C. **1999**. Nucleoside hydrolase from *Leishmania major*. Cloning, expression, catalytic properties, transition state inhibitors, and the 2.5-Å crystal structure. *J Biol Chem* 274: 21114-21120.
9. Arivett, B., Farone M., Masiragani R., Burden A., Judge S., Osinloye A., Minici C., Degano M., Robinson M., and Kline P. C. **2014**. Characterization of inosine–uridine nucleoside hydrolase (RihC) from *Escherichia coli*. *BBA- Proteins and Proteomics* 1844:656-662.
10. Iovane, E., Giabbai B., Muzzolini L., Matafora V., Fornili A., Minici C., Giannese F., and Degano M.. **2008**. Structural basis for substrate specificity in group I nucleoside hydrolases. *Biochemistry* 47:4418-4426.
11. Parkin, D. W., Horenstein B. A., Abdulah D. R., Estupinan B., and Schramm V. L. **1991**. Nucleoside hydrolase from *Crithidia fasciculata*. Metabolic role, purification, specificity, and kinetic mechanism. *J Biol Chem* 266:20658- 20665.

12. Donald V., Judith G. V., Charlotte W. P. Fundamentals of Biochemistry, Third ed. Pg. 378.
13. Versées W., Decanniere K., Pellé R., Depoorter J., Brosens E., Parkin D.W., Steyaert J. **2001**. Structure and function of a novel purine specific nucleoside hydrolase from *Trypanosoma vivax*. *J Mol Biol.* 307(5):1363-79.
14. Petersen, C., and Moller L. B. **2001**. The RihA, RihB, and RihC ribonucleoside hydrolases of *Escherichia coli*. Substrate specificity, gene expression, and regulation. *J Biol Chem* 276:884-894.
15. Versees, W., and Steyaert J. **2003**. Catalysis by nucleoside hydrolases. *Curr Opin Struct Biol.*13:731-738
16. Gault G., Weill FX., Mariani-Kurkdjian P., et al. **2011**. Outbreak of haemolytic uraemic syndrome and bloody diarrhoea due to *Escherichia coli* O104:H4, south-west France. *Euro Surveill*16:19905-19905.
17. Taormina P. J., Beuchat L.R., Slutsker L. **1999**. Infections associated with eating seed sprouts: an international concern. *Emerg Infect Dis*; 5:626-63.
18. <http://www.cdc.gov/ecoli/centers of disease control and prevention>.
19. Gopaul D. N., Meyer S. L., Degano M., Sacchettini J. C., Schramm V. L. **1996**. Inosine-uridine nucleoside hydrolase from *Crithidia fasciculata*. Genetic characterization, crystallization, and identification of histidine 241 as a catalytic site residue. *Biochemistry* 35(19): 5963-70
20. Michael R.H., Gert D. **2005**. Purification and characterization of RihC, a Xanthosine-inosine-uridine-adenosine-preferring hydrolase from salmonella enteric serovar typhimurium. *Biochim Biophys Acta*: 723(1-3):55-62.
21. Giabbai, B., Degano, M. **2004**. Crystal structure to 1.7Å of the *Escherichia coli* pyrimidine nucleoside hydrolase YeiK, a novel candidate for cancer gene therapy. *Structure*, 12:739-749.
22. Berg J. M., Tymoczko J. L., Stryer L. **2002**. The Michaelis-Menten model accounts for the kinetic properties of many enzymes. *Biochemistry*. 5th edition. New York: W H Freeman;Section 8.4.
23. Bornhorst, J. A., & Falke J. J. **2010**. Purification of proteins using polyhistidine Affinity tags. *Methods Enzymol.* 2000; 326: 2445-254.
24. Farone, A., Farone M., Kline P., Quinn T., and Sinkala Z. **2010**. A practical approach for computing the active site of the ribonucleoside hydrolase of *E. coli* encoded by rihC. *Adv Exp Med Biol.* 680:437-443.

25. Ali A., Damanhour G., et al. **2014**. Docking studies of pakistani HCV NS3 hlicase: A possible antiviral drug target. *PLoSONE* 9(9): e106339.doi:10.1371/journal.pone.0106339.
26. Hunt, C., Gillani N., Farone A., Rezaei M., and Kline P. C. **2005**. Kinetic isotope effects of nucleoside hydrolase from *Escherichia coli*. *BBA-Proteins & Proteomics* 1751:140-149.